AN MR-SAFE NITINOL GUIDEWIRE DESIGN FOR INTRAVASCULAR APPLICATIONS

by

Burcu Başar

Bachelor of Science, Biomedical Engineering, Drexel University, 2009

Submitted to the Institute of Biomedical Engineering
in partial fulfillment of the requirements
for the degree of
Master of Science
in
Biomedical Engineering

Boğaziçi University
2015

ACADEMIC ETHICS AND INTEGRITY STATEMENT

I, Burcu Başar, hereby certify that I am aware of the Academic Ethics and Integrity Policy issued by the Council of Higher Education (YÖK) and I fully acknowledge all the consequences due to its violation by plagiarism or any other way.

Name: Burcu Başar Date: 2 June 2015

Signature:

ACKNOWLEDGMENTS

This work is a collaboration between Bogazici University and the Interventional Cardiovascular MRI Catheterization Lab at the National Heart, Lung and Blood Institute, a branch of the National Institutes of Health. The author would like to thank Ahmet Turan Talas at Bogazici University Center for Life Sciences and Technologies for his support during construction of the design prototype, and the interventional MRI catheterization team led by Dr. Robert Lederman at the NHLBI for the technical support and guidance provided during bench tests and animal experiments. Lastly, the author would like to extend gratitudes to Özgür Kocatürk for the opportunity and guidance.

ABSTRACT

AN MR-SAFE NITINOL GUIDEWIRE DESIGN FOR INTRAVASCULAR APPLICATIONS

Magnetic resonance imaging (MRI) offers excellent soft tissue contrast and radiation free imaging. Conventional guidewires employ long metallic materials for versatility and mechanical characteristics, and are subject to RF-induced heating, therefore are inappropriate for use in MR. This work describes the design and testing of a metallic guidewire that is intrinsically MR-safe with preserved mechanical performance.

The MR-safe guidewire was constructed using nitinol rod segments less than a quarter wavelength of RF transmission at 1.5 T within the body to eliminate standing wave formation, hence RF heating. The insulated nitinol segments were connected by short nitinol tubes for a stiffness-matched guidewire core. Mechanical integrity was tested in vitro according to ISO standards. RF-safety was evaluated in vitro according to ASTM standards, and in vivo in swine in a 1.5T MR system. Tests were performed on the prototype and a commercially available guidewire (Glidewire, Terumo, Japan) for comparison. Mechanical tests demonstrated that the segmented-core guidewire behaves similarly to its comparator. In vitro and in vivo RF heating tests confirmed that RF heating is under 2°C as required by US Food and Drug Administration.

The feasibility of an intrinsically safe passive metallic MRI guidewire design is demonstrated. The prototype exhibits negligible heating at high flip angles in conformance with FDA guidance documents ($<$2°C), yet mechanically resembles a high-performance conventional metallic guidewire. This may represent a significant advance once applied to clinical MRI catheterization.

Keywords: Interventional MRI, intravascular guidewire, RF-safety, catheterization.

ÖZET

İNTRAVASKÜLER APLİKASYONLAR İÇİN MR GÜVENLİ NİTİNOL KILAVUZ TEL TASARIMI

Manyetik rezonans görüntüleme (MRG), mükemmel yumuşak doku kontrastı ve radyasyonsuz görüntüleme imkanı sunar. Geleneksel kılavuz tellerde kullanılan uzun, metal malzemeler RF kaynaklı ısınmaya tabidir, dolasısıyla MR altında kullanılamazlar. Bu çalışmada, özünde MR güvenli, mekanik performansını koruyan metal bazlı kılavuz tel tasarımı ve testleri anlatılmaktadır.

MR güvenli kılavuz tel, duran dalga oluşumunu dolayısıyla RF kaynaklı ısınmayı yok etmek amacıyla, vücut içinde 1.5 T altında RF iletim çeyrek dalga boyundan kısa nitinol parçalar kullanılarak üretilmiştir. Elektriksel yalıtım sonrasında bu parçalar, kısa nitinol tüpler ile birleştirilerek kılavuz tel çekirdeğinin sertliği korunmuştur. Mekanik bütünlük ISO standartlarına göre; RF güvenliği, domuz üzerinde in vivo (1.5 T) ve ASTM standartlarına göre in vitro değerlendirilmiştir. Testler, karşılaştırılabilirlik için prototip ve mevcut bir kılavuz tel (Glidewire, Terumo, Japonya) ile yapılmıştır. Mekanik testler, segmente çekirdekli kılavuz telin rakip ürün ile kıyaslanabilirliğini göstermiş; in vitro ve in vivo RF ısınma deneyleri ABD Gıda ve İlaç İdaresi ile uyumlu olarak ısınmanın 2°C'nin altında olduğunu doğrulamıştır.

Bu çalışmada, kendiliğinden güvenli, pasif, metal bazlı MRG kılavuz teli tasarımının uygulanabilirliği gösterilmiştir. Prototip, FDA ile uyumlu olarak, yüksek sapma açılarında dahi önemsiz ısınma (<2°C) sergiler. Mekanik açıdan yüksek performanslı konvansiyonel metalik kılavuz teller ile kıyaslanabilirdir. Bu tasarım, klinik MR kateterizasyon uygulamalarında önemli bir ilerlemeyi temsil etmektedir.

Anahtar Sözcükler: Girişimsel Manyetik Rezonans Görüntüleme, intravasküler kılavuz tel, RF güvenligi, kateterizasyon

TABLE OF CONTENTS

LIST OF FIGURES

LIST OF TABLES

LIST OF SYMBOLS

λ	Wavelength
σ	Standard deviation
ϵ	Permittivity

LIST OF ABBREVIATIONS

MRI	Magnetic Resonance Imaging
XRF	X-ray Fluoroscopy
iMRI	Interventional Magnetic Resonance Imaging
RF	Radiofrequency
ISO	International Organization for Standardization
FDA	Food and Drug Administration
CE	Conformite Europeene
SNR	Signal-to-Noise Ratio
CAD	Computer Assited Design
bSSFP	Balanced Steady State Precession
TR	Repetition Time
TE	Echo Time
FOV	Field of View
SAR	Specific Absorption Rate
CNR	Contrast-to-Noise Ratio
SI	Signal Intensity
GRE	Gradient Echo

1. INTRODUCTION

1.1 Overview

Magnetic resonance imaging (MRI) is potentially an attractive alternative to X-ray fluoroscopy (XRF) to guide interventional procedures due to its superior soft tissue imaging capabilities, lack of ionizing radiation, the integration of arbitrary viewing planes, and user-selected contrast capabilities [1, 2, 3, 4, 5]. The pronounced advantage of interventional MRI (iMRI) over conventional fluoroscopic interventions is the ability to view the interaction of devices with the surrounding tissue in real time [6]. Routine implementation of iMRI to the clinic may enable a wide range of therapeutic applications that are not currently possible with XRF guided interventions, including treatment of congenital heart disease, vascular obstruction, abdominal aortic aneurysm, and targeted myocardial cell delivery [7]. Unfortunately, despite its numerous advantages and demonstrated technical feasibility [8], diagnostic or interventional cardiac catheterization using MRI is not yet commonly deployed [3, 6, 7, 9]. The main obstacle is the unavailability of MRI-safe, conspicuous, and mechanically satisfactory catheterization devices [6, 7, 9, 10, 11, 12, 13, 14, 15, 16, 17]. Commercial guidewires contain long metallic components for mechanical performance, conspicuity under XRF, and cost-efficiency. However, metals that are conventionally used in the construction of catheterization devices are predisposed to radiofrequency (RF) induced heating under MR [1, 3, 7, 9, 11, 13, 14, 18, 19, 20, 21, 22, 23, 24] because of standing wave formation along the conductive parts.

As excessive heating of an interventional device within the body poses a health hazard to the patient, engineering MRI safe guidewires remains a critical problem to be solved. Recent approaches to overcome RF-safety issues intrinsic to the physics of MRI include design of active catheterization devices that implement RF chokes or transformers to constrain RF-induced heating [25, 26, 27, 28, 29, 30]. Other approaches include design of passive intravascular devices that avoid the use of metallic materials altogether to eliminate RF-induced heating due to standing waves along the metallic parts [10, 12, 31]. A detailed overview of the

current attempts at the design of MR-safe catheterization devices is described in Section 1.4. Despite the numerous efforts, however, none of the designs so far have been applicable to the clinic due to the mechanical impracticality of the proposed designs [10, 12]. Consequently, MRI catheterization today remains a feasible yet a largely unavailable clinical application [6, 7]. It is expected that advances in medical device design for the MRI environment will enable both diagnostic interventional MRI catheterization within the next few years [6]. The aim of the work presented here is to describe and demonstrate the design, construction, and feasibility tests of aclinical-grade MR-safe metallic guidewire design that is intrinsically RF- and MR-safe during MRI catheterization.

1.2 Intravascular Catheterization

While a full description of intravascular catheterization techniques is beyond the scope of this thesis, the general concept, the instruments used during catheterization operations, and their limitations as applicable to this work will be briefly explained in this section. Intravascular catheterization is a minimally invasive alternative to open chest surgery for diagnostic and interventional procedures. Catheterization technique was being studied as early as the late 19th century, and by the late 1920's was developed for diagnostic treatment under XRF [32, 33]. Catheterization is performed by introducing catheterization devices, namely, guidewires and catheters, into the patients vasculature through the femoral or radial artery. Upon introduction of guidewires and subsequently catheters into the vasculature, these devices are guided to specific areas in the body, such as the heart or the kidneys, and manipulated as needed at the desired location within the body for diagnostic purposes or delivery of treatment [34].

Cardiac catheterization is performed under XRF, during which contrast agents are used to enhance visualization of the vasculature and catheterization devices [32]. Operational success is therefore highly dependent on the capabilities of the imaging modality as well as the quality of the instrument used during the procedure. XRF allows for two dimensional imaging of anatomical structures, and offers good spatial resolution [9]. However, its ionizing nature has raised

safety concerns for both patients and clinical staff [5, 7, 8, 9]. This becomes particularly disadvantageous during pediatric catheterization, as pediatric patients are at more risk of suffering the potential long term effects than adults under XRF [8]. Therefore, even though intravascular catheterization is a minimally invasive alternative to open heart surgery, it is not always considered a preferred alternative to surgery in children [35].

In the recent years, however, MRI has emerged as an attractive, capable imaging modality. A vast amount of research is focused on the applicability of intravascular catheterization under magnetic resonance imaging, which is radiation-free, offers excellent soft tissue contrast, user-selective slice selection, three-dimensional imaging capabilities; all of which are features of MRI advantageous over XRF[1-5]. In spite of its advantages and technical feasibility, iMRI remains uncommon. The main reason that MRI guided catheterization is not widely spread is the unavailability of MR-safe catheterization devices [6, 7].

Guidewires are an essential tool in catheterization [13, 15, 18, 19, 24]. International Standard ISO 11070 [36] defines a guidewire as a "flexible device over which at catheter or dilator is passed to assist in the insertion and location of the catheter or dilator into a blood vessel" (Figure 1.1). The main purpose of a guidewire, therefore, is to provide support for catheters that are advanced over it. In addition, it must be navigable within the tortuous vasculature of human anatomy without causing any trauma. The design of a guidewire is such that the body of the device provides sufficient support for a catheter to be advanced over it inside the vasculature without bending to the point of deformation or kinking. Its dimensions must be compatible with the vasculature of its intended use, as well as with catheters which are advanced over it. The choice of materials used in guidewire construction along with the mechanical design of these instruments allow for balancing and optimizing these requisites.

The mechanical and physical features expected of a guidewire are:

- Length must cover the cumulative distance from the access site to well beyond the lesion, so that access across the lesion will not be lost during the procedure.

- Diameter chosen in relation to the size of vasculature and catheter used.

- Stiffness to provide support and a stable track along the vasculature, and for axial force and rotational torque transmission

- Tip shape and flexibility tip of the guidewire comes in different shapes and configurations depending on the intended use, and is atraumatic so as to not cause damage to the patient.

- Torquability the ability to apply rotational force on the proximal end, and have that torque transmitted to the distal end of the device to achieve control of the distal end

- Trackability refers to the ability of the guidewire to follow through a tortuous anatomy without bending, kinking, or pulling out of its intended location

- Steerability is the ability to position the tip of the guidewire to the desired location

- Visibility must be visible under fluoroscopy and/or MRI to be able to be navigated

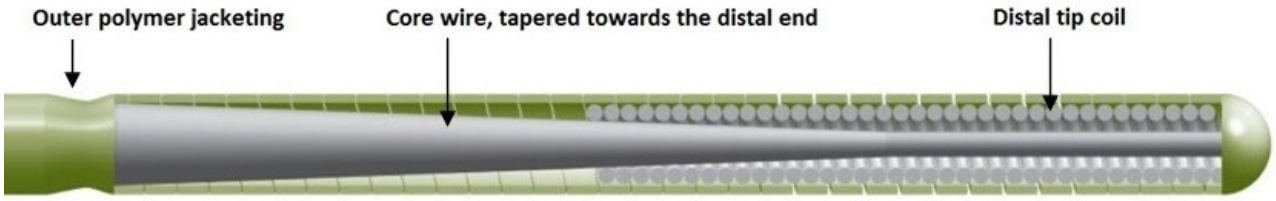

Figure 1.1 Schematic of the distal end of a typical guidewire. A tip coil is typically mounted onto the distal end of the tapered core wire for increased tip performance.

Conventionally, such characteristics are achieved by incorporating metallic components into guidewire design [35]. The core of the guidewire is often made of long, linear, metallic wires, i.e. stainless steel or nickel titanium alloy (nitinol), for good torque response, pushability, kink-resistance, and tensile strength. Another essential guidewire feature is visibility under imaging modality. The same metallic components that provide mechanical features to a guidewire also provide XRF visibility [35]. For enhanced visualization, contrast agents or markers may be utilized during the procedure. However, the ionizing nature of this imaging modality and the nephrotoxicity of the contrast agents pose health hazards for both the patient and physicians [37].

1.3 Interventional Magnetic Resonance Imaging

There has been an immense interest in the use of real-time MRI as a potential alternative to X-ray fluoroscopy as an image-guiding modality for intravascular interventions because of its many capabilities [7, 8, 9]. Interventional magnetic resonance imaging (iMRI) integrates diagnostic and therapeutic procedures in a platform which offers excellent morphological and functional imaging characteristics [9]. The lack of ionizing radiation of the MR environment is another favorable aspect of this imaging modality. The promising concept of iMRI is applicable to many medical fields and may enable new techniques ranging from biopsies and intraoperative guidance to thermal ablation modalities and vascular interventions not available using XRF [8, 9]. Despite its potential advantages, its applicability to catheterization remains delimited by factors intrinsic to the physics of MRI. The challenge is that the components conventionally used in catheterization devices, such as stainless steel and nitinol, are predisposed to radiofrequency (RF) induced heating under MR [4, 10, 11, 12, 13, 14, 16, 17, 18, 19, 20, 21, 23, 24] and risk health hazards to the patient, i.e. blood coagulation, burns. MRI catheterization, therefore, is not yet widely adopted, but is a clinical reality in specialized centers in the United States and Europe [6]. With the rapid development of MRI technology an immense amount of research has focused on MR-safe instruments for interventional procedures [6, 7, 8, 9].

1.3.1 MR-Safety Concerns

Although the potential benefits of MRI are numerous, there exist hazards intrinsic to the physics of MRI that are relevant to diagnostic and interventional catheterization procedures.These hazards may be attributed to the three main components of the MR environment: the static magnetic field, pulsed gradient magnetic fields, and pulsed RF fields [38]. While the direct interactions between the aforementioned fields and the human body are inconsequential, it is the interactions of these fields with medical devices placed within them that create concerns for safety. Table 1.1 provides a summary of the hazards and the relevant concerns related to medical devices in a MR

environment.

Table 1.1
MR Environment Medical Device Concerns. [38]

Component of MR Environment	**Concern**	**Potential Adverse Effect**
Static Magnetic Field (always on)	Rotational force (torque) on object	Tearing of tissues. Rotation of object in order to align with field
Static Magnetic Field Spatial Gradient (always on)	Translational force on object	Tearing of tissues. Acceleration of object into bore of magnet "missile effect"
Gradient Magnetic Field (pulsed during imaging)	Induced currents due to dB/dt	Device malfunction or failure
Radiofrequency Field (pulsed during imaging)	RF induced currents resulting in heating	Patient burns (thermal and electrical)
	Electromagnetic Interference- active device	Device malfunctions. Induced noise (monitoring devices)

Standard guidewires used in interventional procedures to guide the catheter through the arterial system conventionally have a nitinol or a stainless steel core to impart adequate mechanical characteristics to the guidewires. However, guidewires risk RF-induced heating because of the electric currents produced by the RF pulses in and around the conductors in the MR scanner [17]. Furthermore, the use of ferromagnetic materials such as stainless steel risks RF-induced torqueing and displacement of the guidewire when in the vicinity of the magnetic field of the scanner. Therefore, regulatory guidelines impose certain safety standards to limit and control the use of medical devices under MR.

1.3.2 FDA Safety Guidelines For A Medical Device

Medical devices are required to be approved for commercial marketing for use in clinics by the Food and Drug Administration (FDA) in the United

States and Conformité Européenne (CE) in Europe. FDA and CE categorize medical devices depending on compatibility with the MR environment as (1) MR-unsafe, (2) MR-conditional, or (3) MR-safe. In order for a device to be cleared for marketing for use in an MR environment within the scope of its intended use, these governmental bodies require proof indicating that the device is MR-conditional or MR-safe. Device manufacturers must identify their device into one the above categories, and provide a scientific rationale or supporting test data for its approval.

According to FDA [39], "The main issues affecting the safety and compatibility of passive implants in the MR environment concern magnetically induced displacement force and torque, radio frequency (RF) heating, and image artifacts. The static magnetic field of the MR system induces displacement forces and torques on magnetic materials... RF heating in the body is created by currents induced by the RF excitation pulses applied during MR scanning...The presence of an implant may produce an image artifact that may appear as a void region or as a geometric distortion of the true image. If the image artifact is near the area of interest, the artifact may make the MR scan uninformative or may lead to an inaccurate clinical diagnosis, potentially resulting in inappropriate medical action."

Devices that incorporate non-ferromagnetic conducting wires, such as a nitinol-based guidewire, avoid the risk of RF-induced torque and displacement, but risk RF-induced heating. The following additional factors and guidelines are relevant:

"...

RF Heating

...evidence may be submitted that RF heating is insufficient to produce a core temperature increase in excess of 1 degree centigrade, or localized heating to greater than 38 degrees in the head, 39 degrees in the trunk and 40 degrees in the extremities *.

..." [39].

It may be inferred from the guidelines listed here that, when designing a

guidewire for operation under MR, the design should be carefully reviewed and tested for MR and RF safety according to the applicable standards and guidelines. By definition, an MR-safe device poses no risk to the patient if operating under MR environment, and has been demonstrated to neither significantly affect the quality of the diagnostic information nor have its operations affected by the MR scanner [38]. Furthermore, evidence must be provided to show that the localized heating caused by the device is $<2°C$.

1.4 Current Solutions and Limitations

Conventional guidewires that contain ferromagnetic materials such as stainless steel are distinguishable under MR, but are prone to RF-induced torque, displacement, and heating, therefore cannot be utilized during iMRI procedures. Other standard guidewires that contain ferrimagnetic materials, such as nitinol, do not risk displacement or torque, but are unsuitable for the MR environment because they risk RF-induced heating and are not distinctly conspicuous. In an effort to solve MR-safety problems regarding conventional intravascular devices, researchers focus on designs that are conspicuous and free from RF-induced heating. The different approaches categorize intravascular devices as "passive" or "active", based on the visualization technique used for guiding interventional devices to the target tissues [8, 28, 40], each of which have their own advantages and disadvantages.

1.4.1 Active Devices

Active devices are modified guidewires or catheters that incorporate RF coils or dipole antennae to enhance device visualization under MRI. The utmost advantage of active device visualization is superior conspicuity, fast and robust device tracking, as well as the ability of intravascular imaging [41]. By incorporating receiver coils at the catheter or guidewire tip, high signal-to-noise ratio (SNR) images of the surrounding tissue are obtained [41]. Additionally, active visualization may enable depicting the device in color during anatomic images, or may allow the device to be visualized even

when it lies outside the selected imaging slice [42].

As active intravascular devices require signal transmission that transmits the received MR signal along the catheter [41], the major problem encountered with active techniques is RF heating due to long conducting wires [5]. Several different methods have been proposed to reduce [11, 43] or control [44] RF-induced heating. Some groups have investigated RF chokes and shunts to confine RF heating at the tip [11, 16]. The principle is based on transformers placed along the guidewire (Figure **??**), which splits the long conductive wire into several short non-resonant sections [17]. Though heating was in fact minimized at the tip, it was reported that localized heating occurred at the location of the chokes instead [11]. Alternatively, fully optical systems have been proposed where the conducting wires are replaced with inherently RF-safe optical fibers [41], where RF-induced heating is eliminated, but unfortunately these systems suffer from low SNR.

Another constraint of the active designs, even if they manage minimize RF-heating, is reflected as impaired mechanical performance due to the additional components, such as RF chokes and transformers, that are used in their construction. Such methods require application of extra conducting coaxial layers which significantly alter the mechanical properties (flexibility) of the guidewire [17].

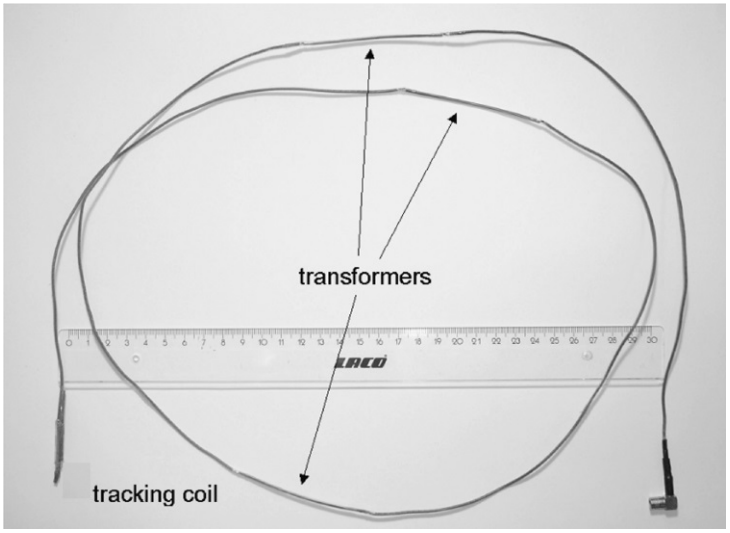

Figure 1.2 An active guidewire design that incorporates transformers along its shaft is shown. The addition of transformers disrupts guidewire profile.

1.4.2 Passive Devices

Passive devices are visualized based on intrinsic material properties [6, 7, 28]. This involves a direct interaction between the physical properties of the interventional device (or the materials used thereof) and the tissue or imaging system [40]. Unlike most active device systems, passive device visualization does not require an external connection to the MR scanner, but simply relies on creating image artifacts with materials embedded in catheterization devices, or utilizes contrast agents [40, 42] to enhance contrast between intravascular devices and the surrounding anatomy. This contrast exists due to the difference in magnetic susceptibility between the contrast material and the surrounding tissue, which creates a local magnetic field inhomogeneity that causes T2* shortening, and consequently, local signal loss [40]. The signal voids may be utilized to locate guidewire location on MR images.

Iron oxide particles, and magnetite in particular, have attracted considerable interest as negative contrast agents due to their excellent magnetic properties, biocompatibility, and biodegradability [45]. Magnetite is a ferrimagnetic material, and primarily alters T_2 values of the water protons surrounding the particle, leading to decreased signal intensity. Consequently, high concentrations of magnetite particles appear dark on MR images [45, 46]. However, these signal voids caused by embedded metals can obscure nearby tissues [8]. In addition, the susceptibility artifact is dependent on the shape of the interventional device, its orientation to the magnetic field, the relative difference of the tissue and device susceptibilities, the orientation of the read and phase axes, and the bandwidth per pixel used to acquire the image [40].

Passive visualization approaches, though attractive in their simplicity and safety in comparison to active devices, suffer poor contrast or excessive artifacts. Although clinical catheterization has successfully been conducted by tracking signal voids using passive catheters, it is therefore less attractive as primary guidewire tracking techniques [7]. In addition, passive techniques unlike active tracking methods, do not offer mitigation of RF-induced heating. To render passive instruments free from heating, research has focused on

replacing the conductive components that exist in conventional guidewires with non-metallic components to eliminate RF induced heating [8, 10, 12]. Visualization of polymer guidewires is accomplished by incorporating embedded metals (or, markers) that can be visualized on the basis of signal voids [8]. In comparison to their metallic counterparts, and similar to the active guidewire designs, however, non-metallic guidewires have been found to have serious shortcomings in terms of their limited mechanical properties, including low torque-response, reduced kink resistance, and difficulty in maneuvering these devices especially within tortuous vasculature during interventional procedures [17].

2. THEORY

2.1 Background

2.1.1 Heat Inducing Mechanisms

An understanding of the underlying mechanisms that cause RF-induced heating is essential to manage MR safety concerns relating to medical devices. According to Maxwell's theory of electromagnetism, there are three mechanisms by which heating can be evoked by RF radiation:

(1) Heating from eddy currents:

As stated by Faraday's induction law, eddy currents are induced in a conductive material by the time-varying magnetic fields. Various studies have investigated heating due to eddy currents [47], concluding that the resultant temperature rises are not significant.

(2) Heating from induction loops:

ECG leads or devices in a looped configuration can pick up RF energy, which results in induced currents, which in turn may cause heating of the material. To reduce the possibility of heating due to induction loops, it is recommended to thermally insulate electrically conductive material in the bore of the magnet from the patient using blankets or sheets [38]. Similar to the heating resulting from eddy currents, the loop effect does not lead to the storage of energy within the device, i.e. the thermal energy is produced directly and instantaneously by the incident RF radiation [17].

(3) Heating by resonating RF waves along conductors:

The most prominent component of RF-induced heating is observed when conductors of sufficient length, such as guidewires, are present in the RF field. According to Maxwell's theory of electromagnetism, the RF magnetic field is surrounded by the RF electric field. Guidewires are long, linear, conductive structures which act like a linear dipole antenna that generates an electric dipole field under MR. RF waves are reflected back and forth along the guidewire forming standing waves,

which subsequently results in an electric current that is induced in the guidewire. Because the induced currents must be zero at the ends of a wire, the law of continuity requires that electric displacement currents occur at these points of discontinuity. At the tip of the wire where the electric field strength is the largest, strong displacement currents are produced within the tissues surrounding the tip. The wire's energy loss then mainly occurs at the wire ends, leading to RF power deposition and potential heating directly at these locations. It is worth noting that the resonating RF waves cause storage of electrical energy along the wire in contrast to mechanisms 1 and 2 [17].

Overall, RF-induced heating is the effect of the interaction between the guidewire and the medium it is in. It depends on a large variety of parameters such as device configuration, position of the device inside the body or the phantom, and geometry of the conductive media the device is in [5, 16, 17, 48]. Due to the non-homogeneous conductive patterns of the human anatomy encountered during interventional procedures, RF power is unevenly distributed in the body and may result in excessive RF energy accumulation in certain locations during an MRI scan [49]. Consequently, when a metallic guidewire is advanced into the close vicinity of these RF-induced hot spots, excessive heating may occur around the neighboring tissues [49]. Additionally, many studies have shown that guidewires induce pronounced heating at the tip [4, 5, 7, 12, 13, 14, 16, 17, 18, 20, 25, 27, 33].

2.1.2 Antenna Theory

Many studies have investigated heating in an MR environment [5, 11, 13, 14, 15, 16, 17, 19, 20, 22, 23, 24, 47, 48, 49]. Excessive heating is mainly attributed to the antennae effect rather than the induced currents [24]. The antenna theory states that the conducting core of the guidewire acts like a linear dipole antenna and the core of a transverse electromagnetic (TEM) waveguide at the same time [17]. To expand on the background given in the previous section, according to Maxwell's laws the RF magnetic field is surrounded by the RF electric field in MR. As a result, when a guidewire of a given length is placed in an MR scanner, a voltage is induced, causing an electric current in the wire. At resonance, the

current reaches a maximum and is distributed along the wire as a standing wave according to Equation 2.1

$$i(z) = i_o cos(\frac{2\pi z}{\lambda}) \tag{2.1}$$

where z is the position of the current in the wire and λ is the wavelength of the RF field. The resistance induced by the surrounding tissue causes an electric loss of power in the wire, hence the guidewire is excited as a dipole antenna that generates an electric field. This field causes eddy current density in the tissue, which occurs in addition to the eddy currents in the tissue by the RF magnetic field. RF power absorption of the guidewire is due to its electric field. Because the induced currents must be zero at the ends of the guidewire, the law of continuity requires that electric displacement currents occur at these points of discontinuity. At the tip of the guidewire where the electric field strength is largest, strong displacement currents are produced within the tissues surrounding the tip. Thus, the power loss is mainly occurring at the wire ends, leading to RF power deposition and potential heating directly at these locations [18].

A number of factors have been shown to affect the amount of heating due to the antenna effect, including physical characteristics of the device such as guidewire diameter and length, as well as those environmental, such as the distance of the guidewire from the isocenter (because coupling occurs between to the electric field of the transmit coil and the guidewire), and the power of the RF pulses [22]. According to the antenna theory the guidewire length required for resonance is an integer of the RF half wavelength in tissue [48], and can be calculated by Equation 2.2:

$$\lambda = \frac{c}{2\sqrt{\epsilon} f} \tag{2.2}$$

where c is the speed of the light ($3x10^8$ m/sec), f is the RF frequency, and ϵ_{tissue} (80) is the tissue permittivity for the human tissue at 64 MHz [50]. This

translates roughly to $\lambda/2$= 21.5 cm in human body at 64 kHz under 1.5T [24]. However, studies conducted on experimental evaluation of the relation between guidewire length and RF-induced heating has yielded results that differ from this theoretical length [24]. Simulations and experimental findings suggest heating attenuation may be optimized at wire lengths less than a quarter wavelength, and more specifically at lengths less than 10 cm [16, 23, 24]. It has been suggested that temperature rise can be minimized for wire lengths measuring less than quarter wavelength at 64 MHz if the insulation thickness is at least 30% of the radius of the wire [24].

2.2 Design Concept

The proposed design relies on the elimination of standing wave formation along the guidewire, which in turn minimizes RF-induced heating along the guidewire. To this end, short metallic rod segments that are unable to resonate at the MRI Larmor frequency are electrically insulated and connected to each other to form a full-length guidewire (Figure 2.1).

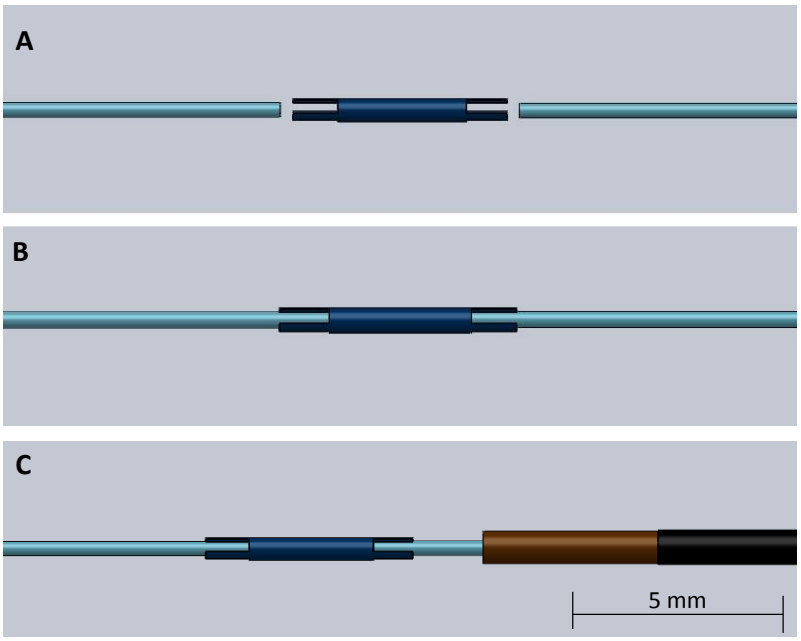

Figure 2.1 The core of the MR-safe segmented guidewire is constructed using insulated 10-cm rod segments and connectors (A), which are interconnected (B) to form a full-length core structure. A 260-cm prototype consists of 25 such connections; which is then jacketed with a polymer-braided tube, and an outer-most layer of thermoplastic polymer is melted over the braided jacketing to complete the device (C).

The length of the non-resonant metallic segments was chosen based on previous studies conducted by Yeung et al [16, 19, 43], where it is shown that RF-induced temperature changes are minimized along wires measuring less than 10 cm with an insulation thickness of at least 30% of the radius of the wire. This length corresponds to less than a quarter wavelength within the human body at 1.5 T.

The insulated metallic segments are adjoined using metallic connectors to preserve the desirable mechanical characteristics of clinical guidewires. Segmentation of the core minimizes RF-induced heating, while implementing stiffness-matched connectors allows for the overall mechanical performance of the guidewire to match that of a commercially available device in terms of pushability, torquability, and tip flexibility. The guidewire design incorporates passive iron oxide markers on its tip and distal shaft to provide MRI conspicuity. The final design is tested for typical mechanical features of a given commercial guidewire for intravascular catheterization applications, namely tip flexibility, torquability, trackability, pushability. MR and RF safety of the device is evaluated in vitro and in vivo. The overall mechanical performance of the final design is tested by simulating the targeted clinical application in vivo in swine.

3. METHODS

3.1 MR-Safe Guidewire Design

3.1.1 Design Specifications

The MR-safe guidewire is intended for use in diagnostic or interventional intravascular catheterization. As MR-safe guidewires are currently not available, the design specifications and performance criteria was based on a commercially available state-of-the-art device (Glidewire, Terumo Inc., Japan) intended for use under XRF guidance (Figure 3.1).

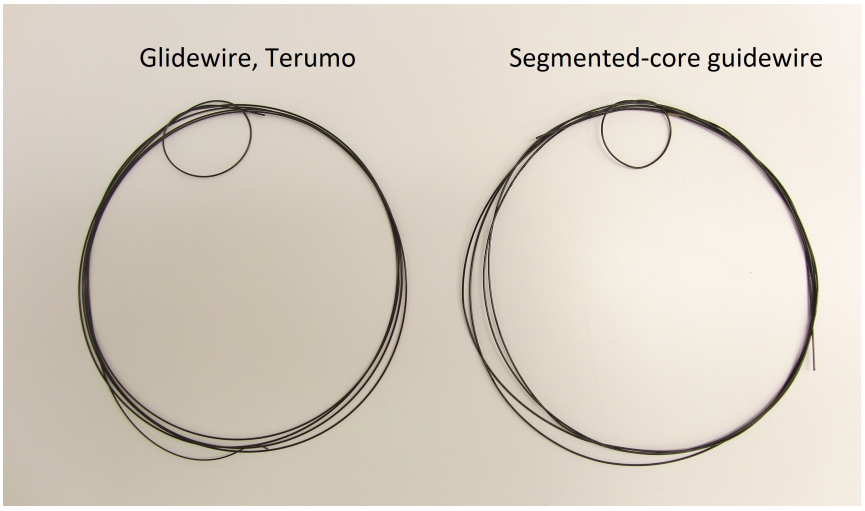

Figure 3.1 A 260 cm commercial Glidewire (left), and a 260 cm segmented-core MR-Safe guidewire prototype (right) in a looped configuration are depicted. Both guidewires exhibit similar bending curvatures at the shaft despite the segmented core structure of the MR-safe guidewire prototype.

In order to test and demonstrate equivalence of the segmented guidewire design to its comparator, the following design specifications were established for the MR-safe design according to ISO 11070 Section 8: Additional requirements for guide wires [36] and FDA's Coronary and Cerebrovascular Guidewire guidance [51]:

- Outer diameter measures 0.035" at the proximal and tapers at its distal tip to 0.032" for increased flexibility. The tapered distal tip is at an angled configuration for steerability (Fig 3.2).

- Effective length of the device is 260 cm, comparable to commercially available XRF guidewires.

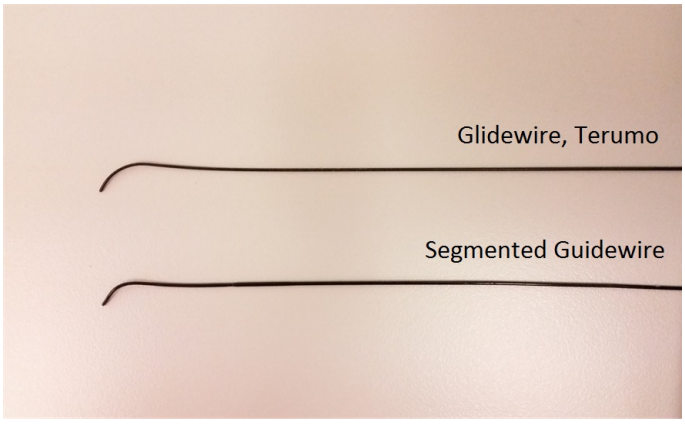

Figure 3.2 A Glidewire (top) and a 260 cm segmented-core MR-Safe guidewire (bottom) exhibit a similar angled profile at the distal tip.

- MR conspicuity of the device is achieved passively based on signal voids.

- RF safety is established such that the device does not cause excessive heating (>2°C in torso), or induce magnetic torque or displacement forces.

To this end, the guidewire should not incorporate ferromagnetic materials that may cause RF induced torque or displacement. Furthermore, it should not incorporate conductive structures measuring more than the quarter wavelength within the body at 1.5T (10 cm) in order to prevent standing wave formation, hence eliminate RF induced heating of tissue under MRI. Additionally, the signal voids caused by the passive markers should not cause excessive obstruction of the anatomical structures in an image, which would yield clinically uninformative images.

3.1.2 MR-Safe Guidewire Construction

The MR-safe guidewire was designed using a computer-aided design (CAD) software (ProEngineer). The initial prototype, including the components and subassemblies, was constructed in an ISO class 7 cleanroom at Bogazici University Center for Life Sciences and Technologies (Instititue of Biomedical Engineering, Istanbul, Turkey).

The guidewire design consists of;

1. A segmented nitinol core;

2. A tapered and angled segment at the distal tip;

3. A polymer braided sleeve over the core;

4. Iron oxide markers for passive visualization; and

5. A final jacketing layer over the marked subassembly that brings the final diameter of the device to 0.035".

Accordiongly, construction of the segmented guidewire prototype follows five steps:

1. Segmented Core Construction

The guidewire core consists of a 0.014" diameter nitinol rod that was segmented into short sections. Each segment measured less than 10 cm, and was coated with a 3-micron parylene film (SCS Inc.) for electrical insulation. The insulated rod segments were then jacketed with a layer of thermoplastic polymer (Pebax, Oscor Inc, Palm Harbor, FL) for increased stiffness. The jacketed nitinol rod segments were interconnected via short sections of a nitinol tube (Figure 3.3).

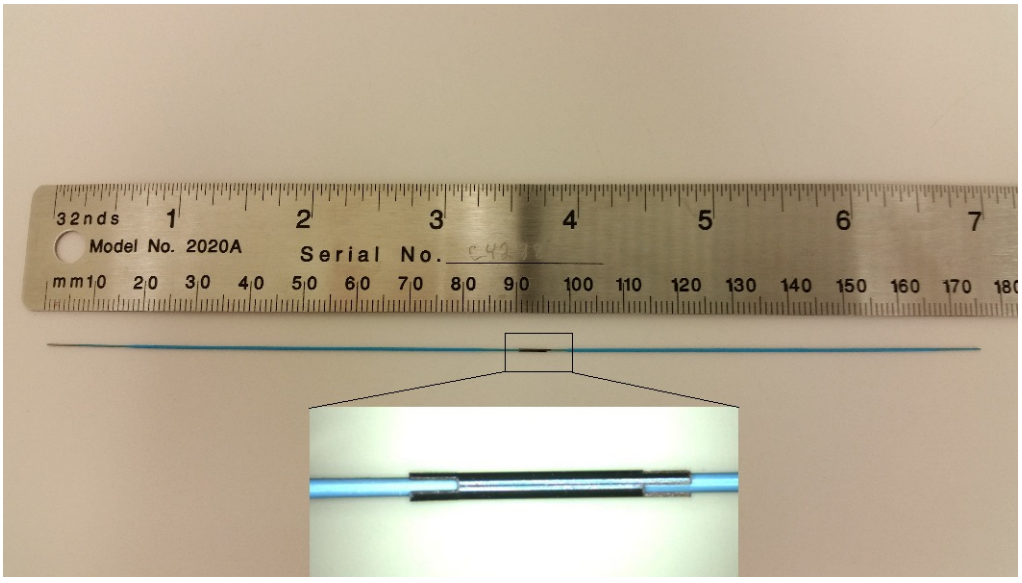

Figure 3.3 Two 10-cm nitinol rod segments are intercnnected using a 5-mm nitinol tube as connector. A full-length guidewire consists of 25 such connections. Pebax jacketing over the rod segments serves as insulation between the rods and the connectors.

The tube sections measure 5 mm in length, and have an inner diameter of 0.016"

and an outer diameter of 0.022" (Fort Wayne Metals, IN). The length of the connector tubes was set at 5 mm based on the bending curvature of commercially available guidewires under microscope (MicroVu, CA). These nitinol connectors were designed using CAD software (ProEngineer) and were cut to 5 mm by Nd:YAG laser cutting system (Lasag Industries Inc., IL).

Two different designs for the connector parts were evaluated during manufacturing:

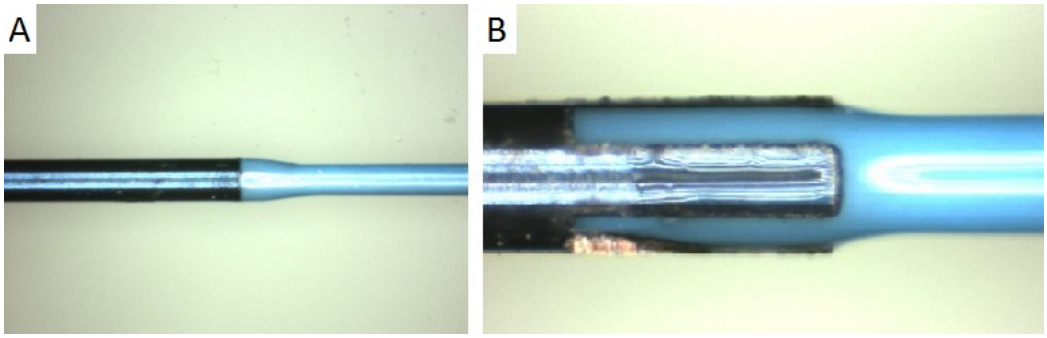

Figure 3.4 An unprocessed connector (A), and a notched connector design are shown (B).

1-Unprocessed connector tubes (Figure 3.4A), and

2-Tubes with a custom notched geometry (Figure 3.4B) that provides increased surface area at the ends of the connector tube for a secure connection between nitinol cores.

The jacketed rods tips were advanced into the laser-cut nitinol connectors from both ends and glued together using a medical grade UV-cured adhesive (Dymax Corporation, Torrington, CT) to create the segmented, non-conducting metallic core of the guidewire (Figure 3.3) that eliminates standing wave formation, hence RF-induced heating.

The layer of thermoplastic polymer (Pebax) jacketed over the rods, which primarily provides stiffness to the nitinol rod segments, also serves to match the diameter of the segments to that of the connectors'. Thus, a profile- and stiffness-matched core structure was constructed such that it appears mechanically indistinguishable from conventional nitinol guidewires while maintaining electrical insulation between segments.

2. Distal Tip of the Guidewire

The distal tip of the guidewire consists of a curved and tapered nitinol rod segment (Figure 3.5). Similar to the components used in guidewire shaft, it measures less than 10 cm to avoid resonance along the conductive nitinol segment.

The geometry of the distal tip segment was based on the comparator guidewire's tip geometry (Figure 3.2).

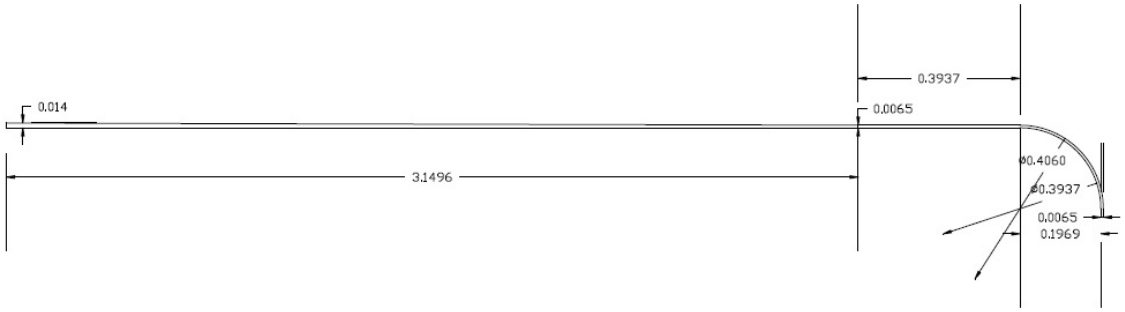

Figure 3.5 The distal tip of the MR-safe guidewire design is illustrated. The curved tip, which provides steerability, is tapered over 5 cm for increased tip flexibility.

1cm It tapers from 0.014" at its proximal end to 0.005" at its distal tip for increased tip flexibility. The angled curve configuration increases guidewire steerability, and also prevents accidental side branch access during use.

The distal tip segment was first insulated with parylene, then jacketed with Pebax similar to the segmented shaft of the guidewire. An insulated solenoid coil (MP35N alloy, Heraeus, MN) which has an inner diameter of 0.028", an outer diameter of 0.032", and is 3 cm in length was attached onto the 0.005" tip of the tapered segment (Figure 3.6). The addition of the coil to the tip serves to maintain the curved shape of the tip, and also matches the reduced distal profile of to the tapered rod to that of the braided sleeve that was advanced over the guidewire shaft, as described in the next subsection. Coil attachment was accomplished by soldering the coil onto the distal tip of the tapered distal segment.

Effect of the solder point on heating and visibility under MRI has been shown to not cause drawbacks previously [44].The distal tip segment, which is electri-

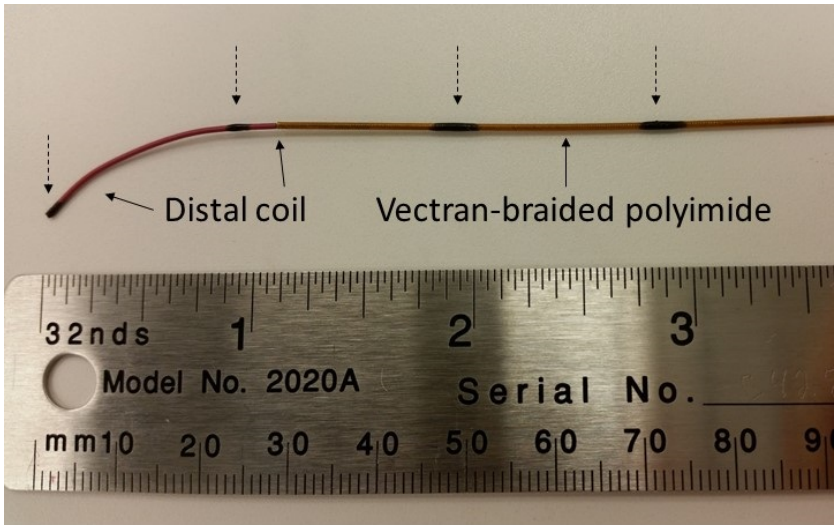

Figure 3.6 The curved and angled distal tip of the segmented guidewire is shown. A 3-cm long coil is mounted onto the curved distal tip of the segmented core. A vectran-braided polyimide sleeve is advanced over the remainder of the segmented core. Iron oxide markers (dashed arrows) are painted over the distal coil and the vectran-braided polyimide layer for passive visualization.

cally insulated, Pebax-jacketed, and incorporates a mechanical coil, was then interconnected to the segmented shaft using the connectors.

3. Polymer Braided Sleeve

A non-metallic fiber (Vectran)-braided (72 ppi, 16 head braider) polyimide tube (0.026" inner diameter, 0.032" outer diameter) was advanced over the segmented core structure, except over the most distal 3 cm of the tip which incorporates a coil (Figure 3.6). This layer of braided sleeve enhances the mechanical capabilities of the guidewire design in terms of pushability, torque response and tensile strength. The non-metallic braiding component of the guidewire provides key qualities that lack in non-metallic MR-safe guidewires, such as kink-resistance, torquability, and stiffness; which in turn provide good support and trackability in vivo.

4. Passive Markers for Passive Visualization

Several types and sizes of iron oxide nanoparticles were evaluated as passive markers for enhanced MR visibility of the MR-safe guidewire design under 1.5T. Iron oxide nanoparticles (Sigma Aldrich, St. Louis, MO) were blended with a UV-cure adhesive (Dymax Corporation) and applied onto the tip coil, and the braided sleeve over the shaft for passive visualization. Markers were applied onto

the distal coil at 1 inch intervals over 5cm. The braided polyimide shaft is marked every 4 inches (Figure 3.6).

5. Final Jacketing

A final layer of thermoplastic polymer (Pebax) was jacketed over the iron oxide marked assembly to bring the outer diameter of the guidewire to 0.035".

3.1.3 Design Variations

The preliminary MR-safe guidewire prototype was 123 cm in length. The distal tip of the guidewire comprised a 13 cm segment, which was the only segment of the whole device that exceeded 10 cm. A second iteration consisted of a shortened distal tip segment measuring less than 10 cm in length, thereby reducing the overall length of the guidewire to 120 cm. All segments of the nitinol core were less than 10 cm in length for the second version. These two preliminary prototypes served as positive and negative control samples, respectively, during heating tests which were conducted in order to confirm that 10-cm segmentation length is in fact effective in eradicating the antenna effect.

3.2 Design Verification Tests

Design verification tests were performed at National Heart, Lung, and Blood Institute (NHLBI)'s Cardiac MRI Catheterization Laboratory (National Institutes of Health, Bethesda, MD, USA). Verification tests consisted of mechanical bench tests and phantom tests as well as in vivo tests.

3.2.1 Mechanical Tests

All mechanical tests were performed based on the test methods listed in FDA Coronary and Cerebrovascular Guidewire guidance document [51] in conformance with ISO 10555-1: 1995 "Sterile, single-use intravascular catheters Part 1: General requirements" [52] in order to obtain in vitro performance data to specify device characteristics in relation to the expected clinical conditions designated for the device. Each test was conducted on at least three samples of test specimen.

Modifications to tests methods were made to circumvent time constraints in relation to prototype construction wherever necessary, without compromising the aim of the test method; i.e., the number of test samples may be reduced without restraining the ability to perform statistical tests on the obtained data. Tests were conducted on segmented guidewires as well as on commercially available nitinol guidewires of matching sizes (Glidewire, Terumo Inc., Tokyo, Japan) for comparability. In vitro tests performed are as follows:

Tensile Strength of the Segmented Nitinol Core

Tensile Strength test aims to "verify that the device and all its joints (adhesive/solder/braze) are sufficiently strong to withstand normal tensile loading for the intended use. Testing should be conducted on at least ten (10) of each of the smallest and largest diameter wires. The test protocol should specify the pull rate used in each test", as described by the relevant ISO standard [52]. The method was modified to perform the test on three (3) subassembly specimens to verify that the overall device maintains its mechanical integrity and is able to withstand tensile forces of at least 5 N as required by the relevant ISO standard [52] for intravascular medical devices.

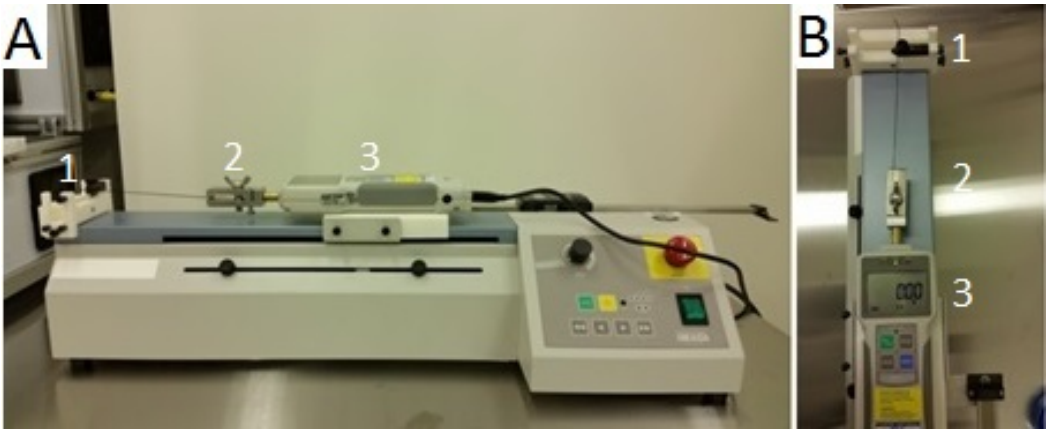

Figure 3.7 (A) Side view and (B) aerial view of the tensile strength test set-up: a test specimen is secured in the stationary jaw (1) and the motorized jaw (2) which pulls at a constant speed while monitoring the tensile forces (3).

Tensile strength tests were performed on five sample groups, each group consisting of five test specimens:

(a) two nitinol rod segments connected with the notched connector,

(b) two nitinol rod segments connected with the unprocessed connector design,

(c) guidewire subassembly consisting of two connected nitinol rod segments jacketed with Vectran-braided polyimide,

(d) intact, non-segmented nitinol rod jacketed with Vectran-braided polyimide,

(e) distal tip with attached coil.

The braided polyimide and final Pebax layers that provide additional support on segmented core were intentionally excluded from test specimens to provide worst-case testing conditions. The subassembly structures were secured on to a stationary jaw on one end and pulled on the other end through a force meter positioned on a motorized linear stage (Imada Inc. Model ZP-11) as shown in Figure 3.7. The force meter was moved away from the subassembly with a constant speed. The force at which the two segments are separated was then recorded.

The tensile strength test was performed on specimens that were prepared using two different nitinol connector designs, namely the notched connector design and the flat connector design. Once the mechanical and structural integrity of the connected segments was established, additional tensile strength tests were conducted on the complete guidewire design.

Attachment Strength of the Distal Tip to the Distal Rod

A distal tip attachment test was conducted on the segmented guidewire prototypes to ensure that the guidewire tip, which lacks the braiding-reinforced sleeve, is able to withstand tensile forces up to, at minimum, 5N as required by the ISO standard [52]. The same test setup as the tensile core strength was used. The proposed guidewire design was further evaluated by testing the soldering attachment strength of the coil onto the distal tip by performing a tensile test.

Tip Flexibility Test

The tip flexibility test aims to demonstrate the force required to deflect the distal tip to a range of angles. Accordingly, the flexibility of the tapered distal tip was evaluated by measuring the deflection force at 5mm, 10mm, and 20mm from the distal tip when it was deflected to various angles (15°, 30°, 45°, 60°) (Figure 3.8).

The force was measured using a low force capacity load cell (IDTE 2000, Machine Solutions Inc., Arizona).

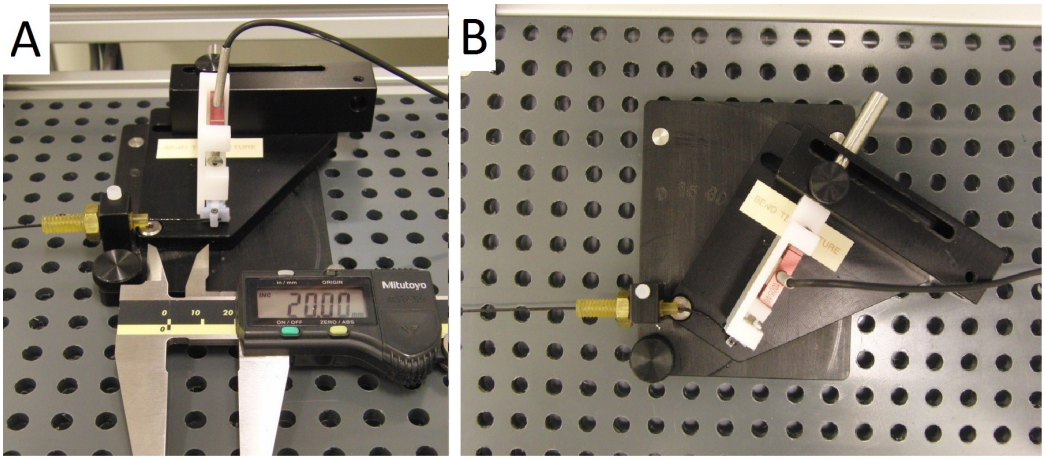

Figure 3.8 Tip flexibility test set-up: The guidewire is placed in a low-capacity load cell fixture at a set distance from the tip, which measures the force required to deflect the tip to various angles. The set distance is 20mm in (A), and the tip is bent to 45° in (B).

Pushability Test

The pushability test was performed on the segmented guidewire and a Glidewire to assess maneuverability performance of the two devices. The force required to advance the guidewires within a custom vascular anatomy model that mimics the left heart catheterization vasculature (Figure 3.9) was measured using the intravascular device testing equipment (IDTE 2000, Machine Solutions, AZ). The test was conducted under dry conditions to compensate for the lack of

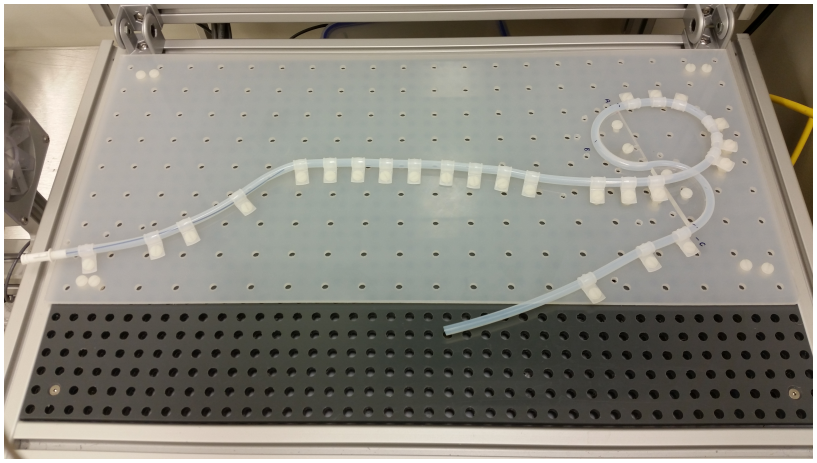

Figure 3.9 Pushability test set-up is shown. The automated equipment advances the guidewire through a vasculature that mimics left heart catheterization trajectory, and records and graphs the forces measured.

hydrophilic coating on the segmented guidewire. IDTE's automatic roller system advanced the guidewires at a set speed of 200cm/min through the aforementioned vascular phantom over a pre-determined distance (65 cm) corresponding to the average distance from femoral artery to the aortic arch.

Torquability Test

Torquability test aims to evaluate the torque transmission capacity of the guidewire from the proximal end to its distal end by correlating the rotation of the proximal end and the corresponding rotation of the distal end of the guidewire. FDA guidelines [51] state that testing should be conducted in a simulated anatomy model on at least five (5) devices. Each test sample was advanced into a custom vasculature model made of PTFE tubing that mimics the right heart cardiac catheterization trajectory (Figure 3.10). The start and end points of each rotation was marked on 360° paper protractors attached to the guidewire on both ends. The distal tip of the guidewire extended beyond the end of the phantom, and was marked with a tape to track the degree of rotation observed at the distal end with each rotation at the proximal end.

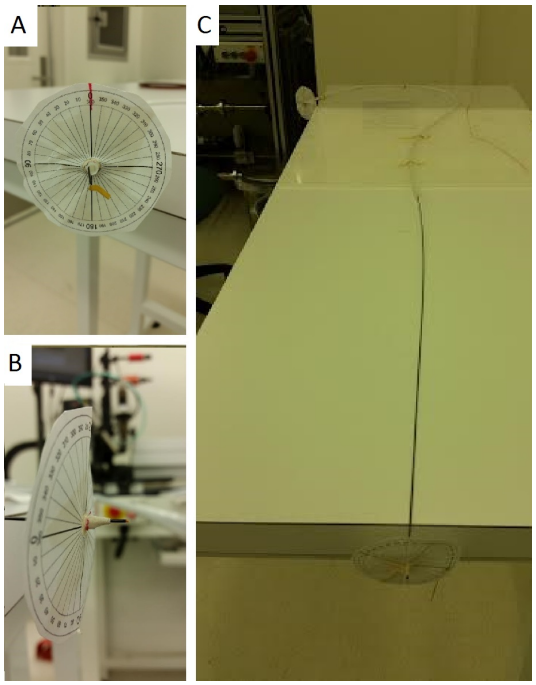

Figure 3.10 Torquability test uses a protractor fixed on the phantom at the distal end, a marker on the guidewire to track the number of rotations observed at the distal end of the guidewire (A); and protractor fixed on the proximal end of the guidewire to track number of rotations applied to the guidewire (B). The guidewire is torqued inside a phantom that mimics the left heart catheterization trajectory (C).

3.2.2 RF-Safety Tests

All tests were conducted on prototypes and a commercially available comparator (Glidewire). An experimental setting that accounts for the various parameters which result in increased RF-induced heating was established to assess heating around the proximity of the MR-safe segmented nitinol guidewire. RF-induced heating depends on a large variety of parameters such as device configuration, position of the device inside the body or the phantom, and geometry of the conductive media the device is in [13, 17, 23, 19]. Due to the non-homogeneous conductive patterns encountered during interventional procedures, RF power is unevenly distributed in the body and may result in excessive RF energy accumulation in certain locations during an MRI scan [49]. Consequently, when a metallic guidewire is advanced into the close vicinity of these RF-induced hot spots, excessive heating may occur around the neighboring tissues. Previous studies show that the hot spot is at the tip of the guidewire [17]. A number of factors have been shown to determine the amount of RF heating due to the antenna effect, including guidewire geometry (diameter and length), distance from the isocenter (because coupling occurs between to the electric field of the transmit coil and the guidewire), and the power of the RF pulses [22]. Worst-case RF induced heating conditions were created during the experiments such that; (1) a high flip angle was chosen (75°, compared with 45° used in a routine interventional MR procedure), (2) a no-flow ASTM 2182 phantom [42] with minimal thermally dissipative properties was used, and (3) the tested guidewire was positioned at an off-center position within the scanner bore, as explained in the following section.

Temperature data was acquired using a fiberoptic temperature probe (OpSens Inc., Canada) with a sensitivity of 0.1°C and an operational range of 0 °C to 85 °C. The probe was fed through a polyimide channel (0.009" ID, 0.011" OD), which was parallel and affixed to the guidewire along its length, using a heat shrink tubing (Advanced Polymers, Salem, NH). The distal tip of the channel extended beyond the distal tip of the guidewire by 1 cm. The channel was sealed using a UV-cure adhesive on tis distal end to prevent inflow of media into the channel. The fiberoptic temperature probe was free to move through this poly-

imide channel during the heating experiments. All heating tests were performed in a 1.5T MR system (Aera, Siemens, Erlangen, Germany) using balanced steady state precession (bSSFP) sequence (TR/TE 2.9/1.4ms; flip angle 45° and 75°; bandwidth 1000Hz/pixel; matrix 192x108; FOV 300x300mm; GRAPPA Factor 2) and gradient echo sequence (TR/TE 4.2/1.9ms; flip angle 15°; bandwidth 500Hz/pixel; matrix 192x144; FOV 300x300mm; GRAPPA Factor 2).

Phantom Set-Up

In vitro RF-induced heating test of the segmented guidewire design was performed by using the ASTM 2182 phantom that has similar electrical properties to that of the human body. The acrylic gel phantom consisting of a polyvinyl container (43cm x 72cm x 21cm) filled with a polyacrylamide gel (6.5% acrylamide, 0.3% bisacrylamide, 0.05% TEMED, 0.08% ammonium persulfate; EM Science, Gibbstown, NJ) doped with 0.45% sodium chloride was prepared according to ASTM 2182 F-02 [42].

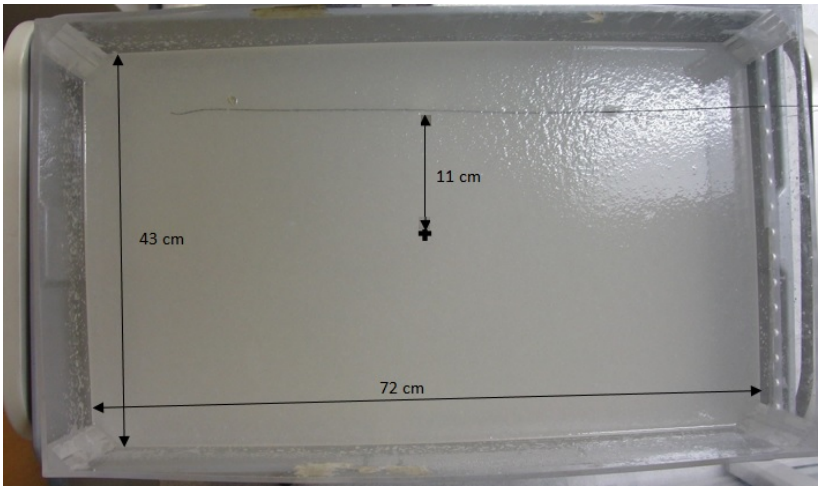

Figure 3.11 ASTM phantom and a guidewire with its tip placed at the hot-spot as during a typical RF-induced heating test. Isocenter of the phantom is shown with '+'.

The guidewire was placed 11-cm off-center at a 6-cm depth in the phantom during the experiments to align with high electric field (E-field) region within the bore in order to create worst-case simulation conditions (Figure 3.11).

Experimental Procedure

Prior to the start of each experiment the geometric center of the phantom was positioned exactly in the center of the scanner bore. The phantom was registered

supine, head first. The temperature probe was placed at the distal end of the channel, which extends beyond the distal tip of the guidewire. The guidewires tip was then positioned at the designated hot-spot of the phantom to ensure maximal heating around the guidewire.

A 30-second temperature recording was taken prior to the initiation of each MR imaging pulse sequence to obtain a baseline temperature of the gel at room temperature. Following this initial 30-second no-scan period, each test sample was scanned for a successive 30-second period during which the probe remains stationary at its initial position, which allows for recording the temperature change of the gel during the scan.

Immediately following the 30-second static probe scan, a probe pull-back test was performed, during which temperature changes along the length of the guidewire were continuously monitored by slowly retracting the temperature probe out of the channel at a constant speed. The probe pull-back test enabled detecting the hottest spot along the guidewire. It also served to evaluate whether heating occurs at the location of each connector along the guidewire, where electrical insulation may be compromised during manufacturing.

The second part of the heating experiment aimed to evaluate temperature changes at the hot spot, specifically, measured through the probe pull-back test. Prior to scanning, the temperature probe was placed at the distal end of the probe channel, and the 30-second no-scan followed by 30-second scan of the static probe steps were completed. Immediately following these initial baseline temperature readings, the probe was pulled to the predetermined hot spot of the guidewire and a 60-second temperature reading at the hot spot was then collected.

Real-time bSSFP sequence was used during the experiment (TR/TE, 2.88/1.44 ms; thickness, 6mm; FOV, 350 $\times$ 350mm; matrix, 192 $\times$ 144). A non-clinical, high flip angle (75°) that did not activate the specific absorption rate (SAR) watchdog was chosen to achieve a high temperature increase, simulating worst-case conditions.

3.2.3 Guidewire Conspicuity Under MR

Conspicuity was achieved by implementing passive iron oxide markers onto the distal shaft of the guidewire. Iron oxide particle samples with a range of core diameters (Sigma Aldrich) were blended with a UV-cure adhesive (Dymax Corporation) and applied onto the guidewire at 1 inch intervals. The effect of varying core sizes on image artifacts was evaluated in vitro (Table 4.2). In vitro images were obtained in a phantom prepared according to ASTM F2119-07 Standard Test Method for Evaluation of MR Image Artifacts from Passive Implants [35] to assess visibility of the device under MR. Device visibility was evaluated by comparing the contrast-to-noise ratio and the susceptibility artifacts created by different types of iron oxide particles in an MR scan. The contrast-to-noise ratio (CNR) of the iron oxide markers was calculated according to Equation 3.1;

$$CNR = \frac{SI_{marker} - SI_{background}}{\sigma_{imagenoise}} \tag{3.1}$$

where; SI_{marker} and $SI_{background}$ are signal intensity of the marker and the image background, respectively, and $\sigma_{imagenoise}$ is the standard deviation of the image noise. Susceptibility artifact caused by the different markers was evaluated according to ASTM-F2119-07 [35].

All MR imaging studies were performed in a 1.5T MRI system (Aera, Siemens, Erlangen, Germany). To assess visibility of the device under MRI, in vitro images were obtained in a 20 x 15 x 10 cm copper sulfate doped water phantom prepared according to ASTM 2182 [42]. The phantom was placed in the center of the scanner, and the samples scanned were placed in the center of the phantom. Device conspicuity was evaluated for GRE (TR/TE, 41/10 ms; thickness, 5mm; FOV, $300x300$ mm; matrix, $128x128$), bSSFP (TR/TE, 2.88/1.44 ms; thickness, 6 mm; FOV, 350×350 mm; matrix, 192×144), and real time gradient echo (TR/TE, 3.0/1.44 ms; thickness, 6 mm; FOV, 350×350 mm; matrix, 192×144) sequences.

3.2.4 In Vivo Catheterization and Heating Evaluation

All animal experiments were conducted at the NIH under the current collaborative research agreement. All experiments were carried out in accordance with the Guide for the Care and Use of Laboratory Animals (NIH Publication no. 80-23, revised 1985) and the principles of Laboratory Animal Care of the National Society for Medical Research. The experimental protocol was previously approved by the Animal Care and Use Committee at the NHLBI. Animals were anesthetized and monitored throughout the experiments. The experiments were performed on sterilized guidewires under sterile conditions.

Cardiac left heart catheterization was performed on a total of seven (n=7; weight=43 ± 17.62 kg) swine using a preliminary protocol to assess RF-induced heating, conspicuity, and qualitative mechanical performance of the device.

During four of the left heart catheterization experiments, RF-induced heating was evaluated.

In vivo RF induced heating experiments were performed using the fiber optic probe placed at the distal tip of the guidewire to monitor RF induced temperature increase. Throughout the experiments, the core temperature (rectal) of the test animal was monitored on a separate channel as baseline core temperature. Temperature change was measured as the instantaneous difference between the temperature at the guidewire tip and the core temperature of the animal. The increase in core temperature of the animal was measured as the difference between the instantaneous core temperature and the average pre-scan core temperature.

Scanning was initiated at t=30 seconds in order to acquire pre-scan baseline data. Catheterization began after initiating scanning in ordder to monitor temperature changes upon femoral access. 60-second stationary temperature data were taken at discrete locations within the test subject's vasculature starting from point of femoral access to aortic arch at 5 cm increments, corresponding to different insertion lengths. Upon reaching the arch, a temperature probe pull-back was performed by retracting the probe out of its channel while holding the guidewire stationary at the aortic arch. This verified that no heating occurs along the shaft of the guidewire while its tip is at the aortic arch.

4. RESULTS

4.1 Mechanical Test Results

Tensile Strength

Results summarized in 4.1 show that the force required to separate two inter-connected core segments is higher for the notched connector design (11.34 ± 2.14 N) than for the flat connector design (8.84 ± 1.74 N), both of which are well above the minimum limit of 5 N indicated by the ISO 10555-1: 1995 standard [52]. When the samples were jacketed with a Vectran-braided outer layer the tensile force required to break the guidewire sub-assembly increased three-folds (30.97 ± 0.20 N) . Similarly, tensile strength tests conducted on a Glidewire has shown that the outer layer breaks at forces above 30 N. The force required to detach the tip coil from the core structure of the segmented guidewire was 19.24 ± 1.30 N based on five test samples.

Table 4.1
Tensile strength test results

	Rod-to-Rod Attachment		**Rod-to-Rod sections (jacketed)**	**Tip coil to distal tip attachment**
	Notched connector	Unprocessed connector		
Force-at-Break (N) (mean±std dev)	11.32 ±2.14	8.84 ±1.74	90.97 ±0.2	19.24 ±1.3

Tip flexibility

The distal tip flexibility of the commercially available Glidewire (Figure 4.1) and the segmented guidewire exhibit similar profiles, but differ in resultant forces measured.

Pushability

Results show similarly pushability profiles between Glidewire and the segmented guidewire (Figure 4.2).

Torquability

Results compare the proximal rotational input and the resulting distal rotation at 90° intervals. The number of rotations applied at the proximal end was plotted against the number of rotations observed at the distal end. The overall torque response the MR-safe segmented nitinol core guidewire is similar to a Glidewire as shown in Figure 4.3.

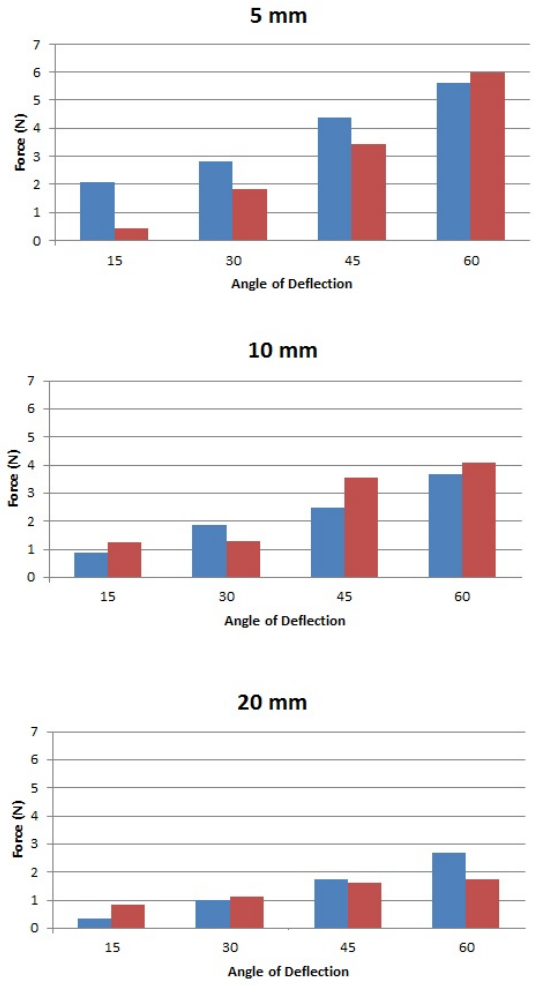

Figure 4.1 In vitro measurement of the tip flexibility of the Glidewire and the segmented guidewire are defined as the force required to deflect the tip to 15, 30, 45, and 60 at 5mm (top), 10mm (middle), and 20mm (bottom) from the tip.

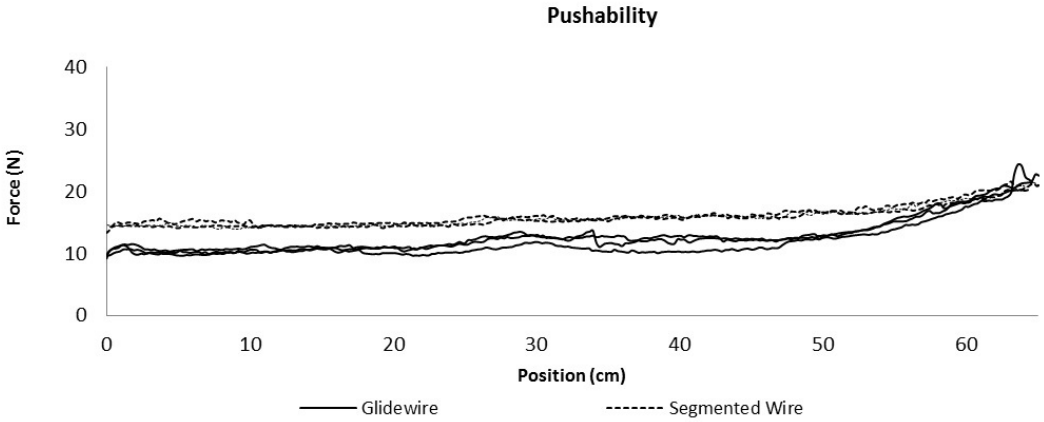

Figure 4.2 In vitro pushability test results show similar profiles between the Glidewire and the MR-safe segmented guidewire.

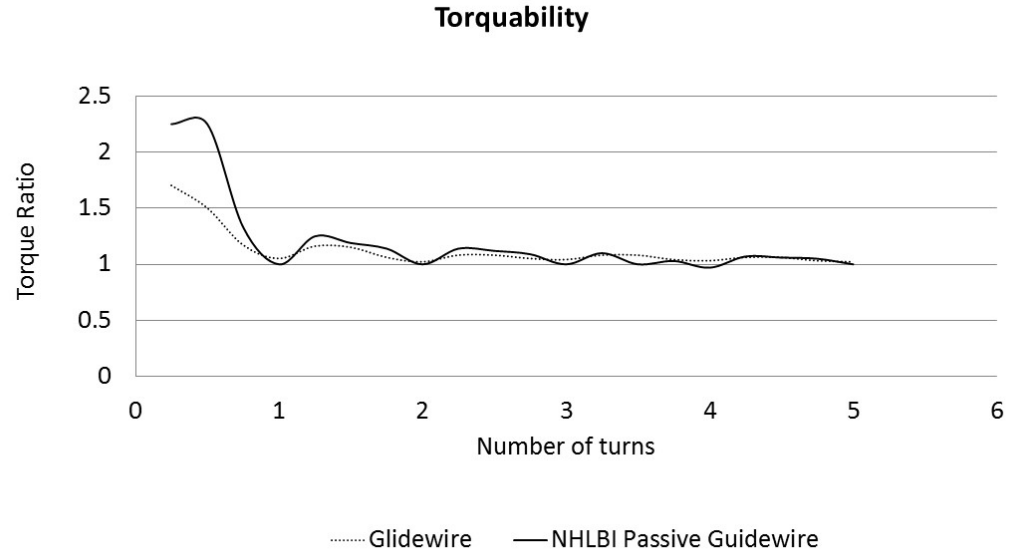

Figure 4.3 In vitro torquability of the Glidewire and the segmented guidewire are depicted.

4.2 In Vitro RF-Induced Heating Tests

In vitro heating test results demonstrate that the temperature increase at the tip of the 123 cm segmented guidewire, which had a 13-cm tip segment, was 3.8 °C compared with 1.6 °C increase measured at the tip of the 120 cm prototype, which had a shortened 10-cm distal tip segment (Figure 4.4).

Further in vitro heating tests conducted on the 260-cm MR-safe segmented guidewire prototype showed that the temperature measured at its tip in-

creased by a mere 1 °C in comparison with the 10 °C increase observed at the tip of a 260-cm Glidewire upon initiation of scanning at a 75° flip anlge.

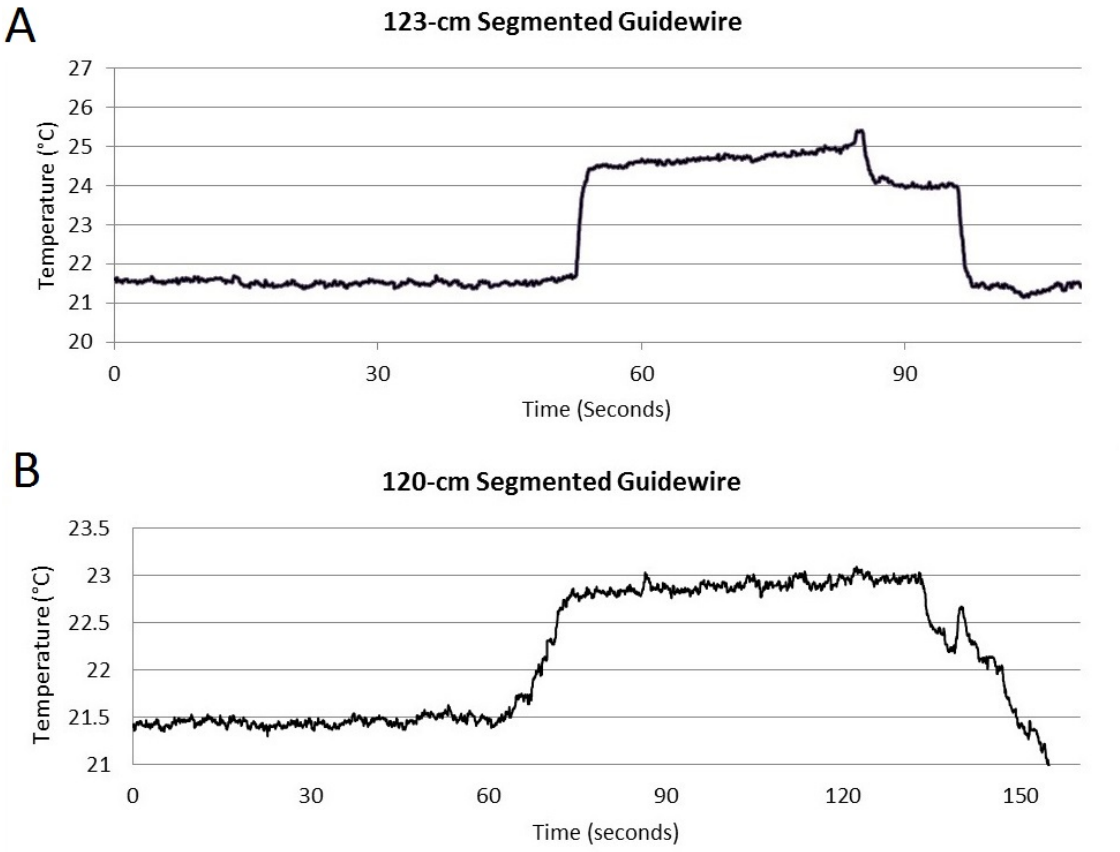

Figure 4.4 Temperature measured at the tip of a 123-cm segmented guidewire (A) and a 120-cm segmented guidewire (B) in a phantom. Scan was initiated at t=30 seconds. Probe was stationary at the tip during t=60-120 seconds. Probe pull-back starts at t=120 seconds, showing temperature changes along the shaft.

At the end of 60 seconds of scanning, temperature at the tip of the Glidewire had increased by 13.4 °C as opposed to 1.2 °C at the tip of the segmented guidewire (Figure 4.5). The maximum temperature recorded during the probe pull-back tests, which followed the 60-second scan at the hot-spot (distal tip), shows that the temperature increase along the shaft of the segmented nitinol guidewire is below 2°C.

Additionally, temperature changes of the phantom in the absence of a guidewire were acquired separately as baseline data (Figure 4.6). Two separate temperature probes measured temperature at the isocenter and at the

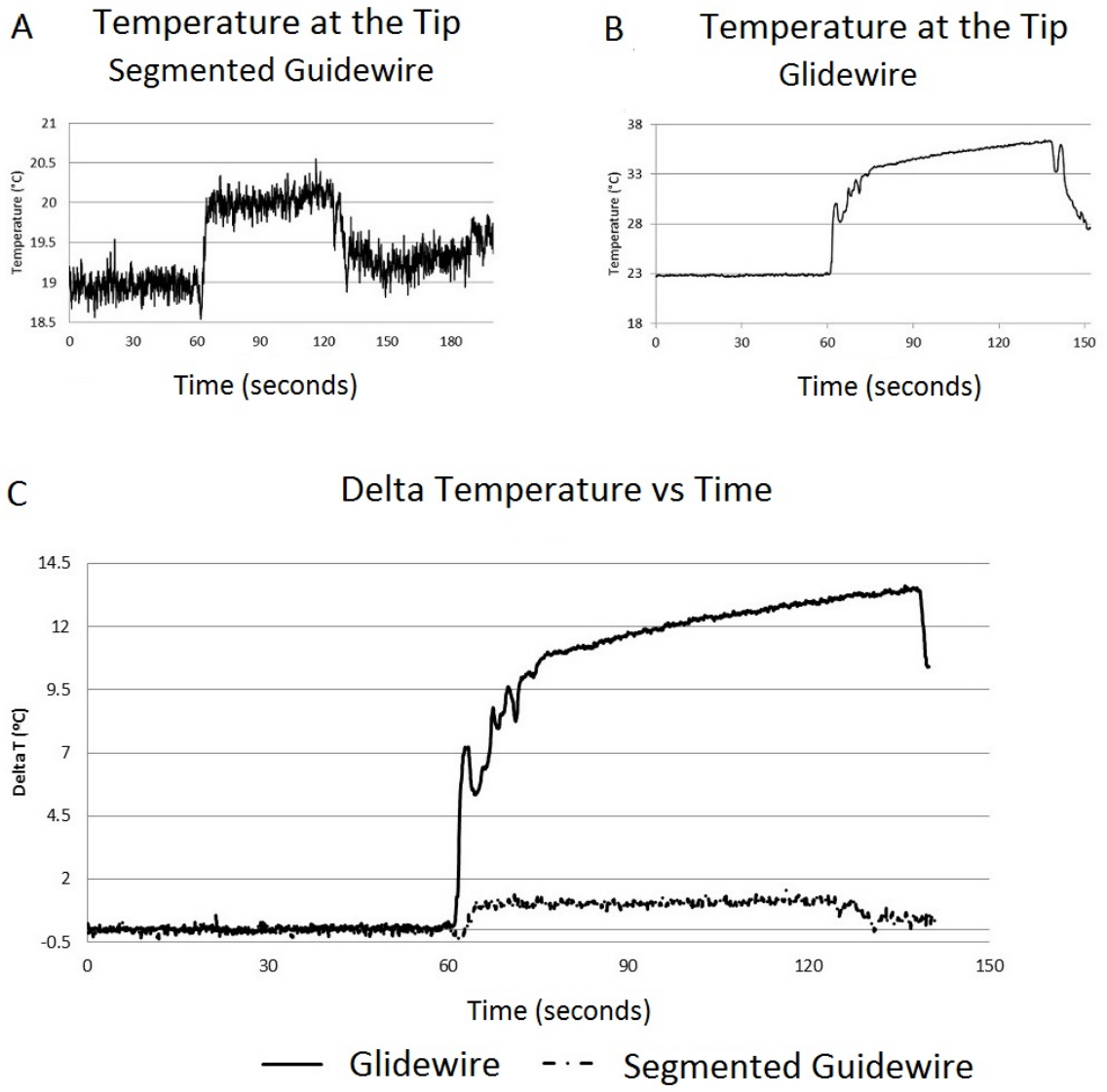

Figure 4.5 Temperature measured at the tip of the 260 cm segmented nitinol guidewire (A) and a 260 cm Glidewire (B) in a phantom. Temperature change at the tips are 1.2°C in comparison with 13.4°C (C). Scan was initiated at t=30 seconds. Probe was stationary at the tip during t=60-120 seconds. Probe pull-back starts at t=120 seconds, showing temperature along the shaft.

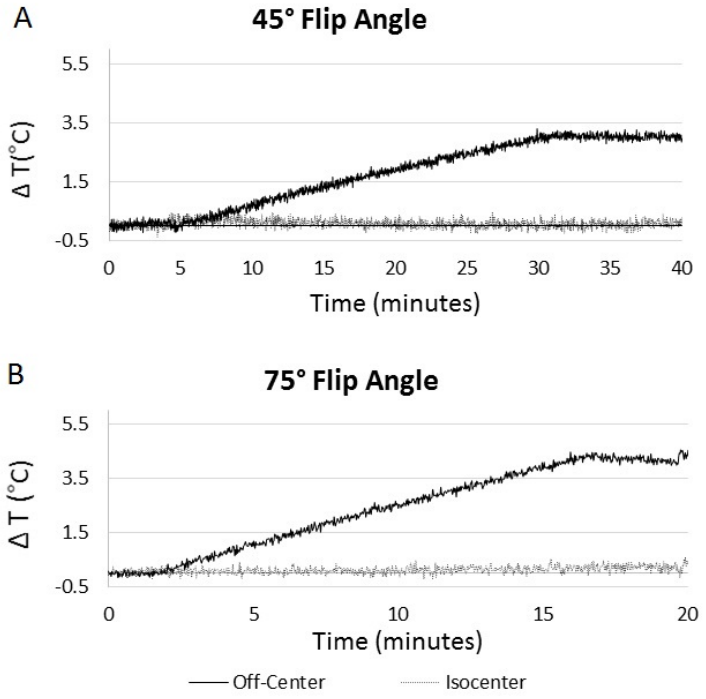

Figure 4.6 Baseline RF-induced heating data acquired during the scan of the phantom alone at a 45°(a) and a 75°(b) flip angle. No conductive materials were present in the phantom.

4.3 Guidewire Conspicuity Under MR

In vitro scans demonstrate the effect of nanoparticle core size on image artifact features (Table 4.2). Markers were evaluated in vitro for resultant susceptibility artifact according to the ASTM standard [42] (Figure 4.7) as well as qualitatively in vivo during left heart catheterization in swine (Figure 4.7).

Table 4.2
Comparison of marker characteristics of magnetite particles with various core sizes

Magnetite core size	50 nm	70-150 nm	5 μm
Susceptibility artifact width (cm)	1.11	1.22	0.52
Contrast-to-noise ratio	45.29	48.79	29.17

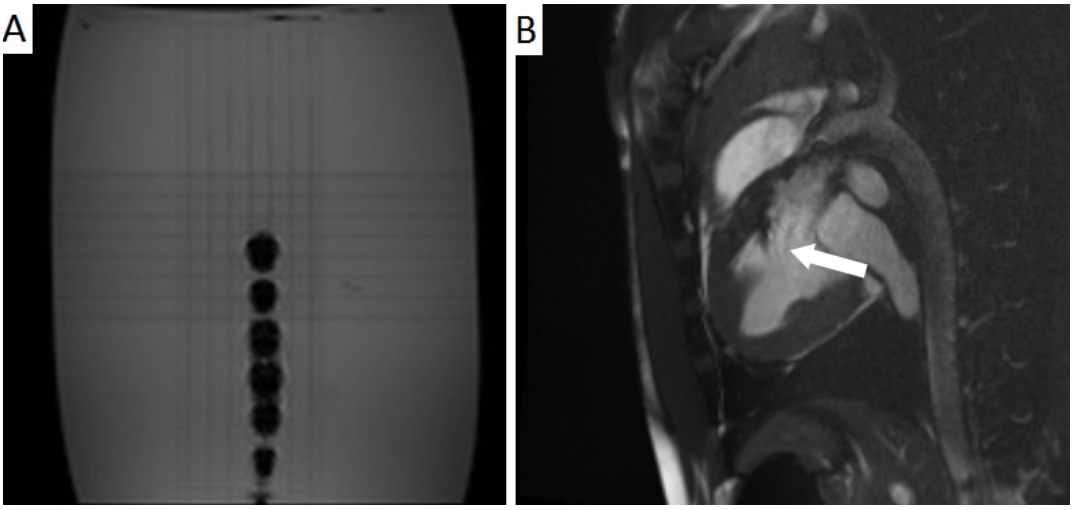

Figure 4.7 (A) In vitro image of the distal tip of the segmented guidewire with magnetite markers (particle core size in the 70-150 nm range) painted onto it. (B) In vivo image acquired during left heart catheterization in swine. Tip of the MR-safe segmented guidewire is shown with white arrow.

4.4 In Vivo Catheterization and Heating Performance

Cardiac left heart catheterization was performed on seven swine. Upon femoral access the guidewire was advanced through an introducer sheath (5F Pinnacle, Terumo) to the aortic arch. The guidewire was found to be steerable, torquable, and conspicuous for successful advancement to the aortic arch in all cases. During one out of seven cases the operator was unable to deliver the device was into the left ventricle.

Heating of the device was investigated during four left heart catheterization procedures (n=4, weight=24-63 kg). Table 4.9 summarizes pre-scan data as well as recorded temperature data acquired from all four animals during the experiments.

No significant heating was observed at the tip of the guidewire or along the shaft of the device (Figures 4.8; 4.9; 4.10; 4.11).

Table 4.3
In vivo heating tests

Experiment number	1	2	3	4	
Animal weight (kg)	58	63	24	27	43.25
Total scan duration (minutes)	35	36.52	30	30	
Time of start of scan (seconds)	60	245	245	70	
Time of guidewire insertion (seconds)	120	300	305	130	
Average pre-scan core temperature (°C)	35.3	35.3	33.9	37.8	35.6
Maximum Δ Core Temperature (°C)	0.8	0.6	0.4	0.6	0.6
Maximum Δ temperature at guidewire tip (°C)	1.2	1.3	0.7	1.3	1.12

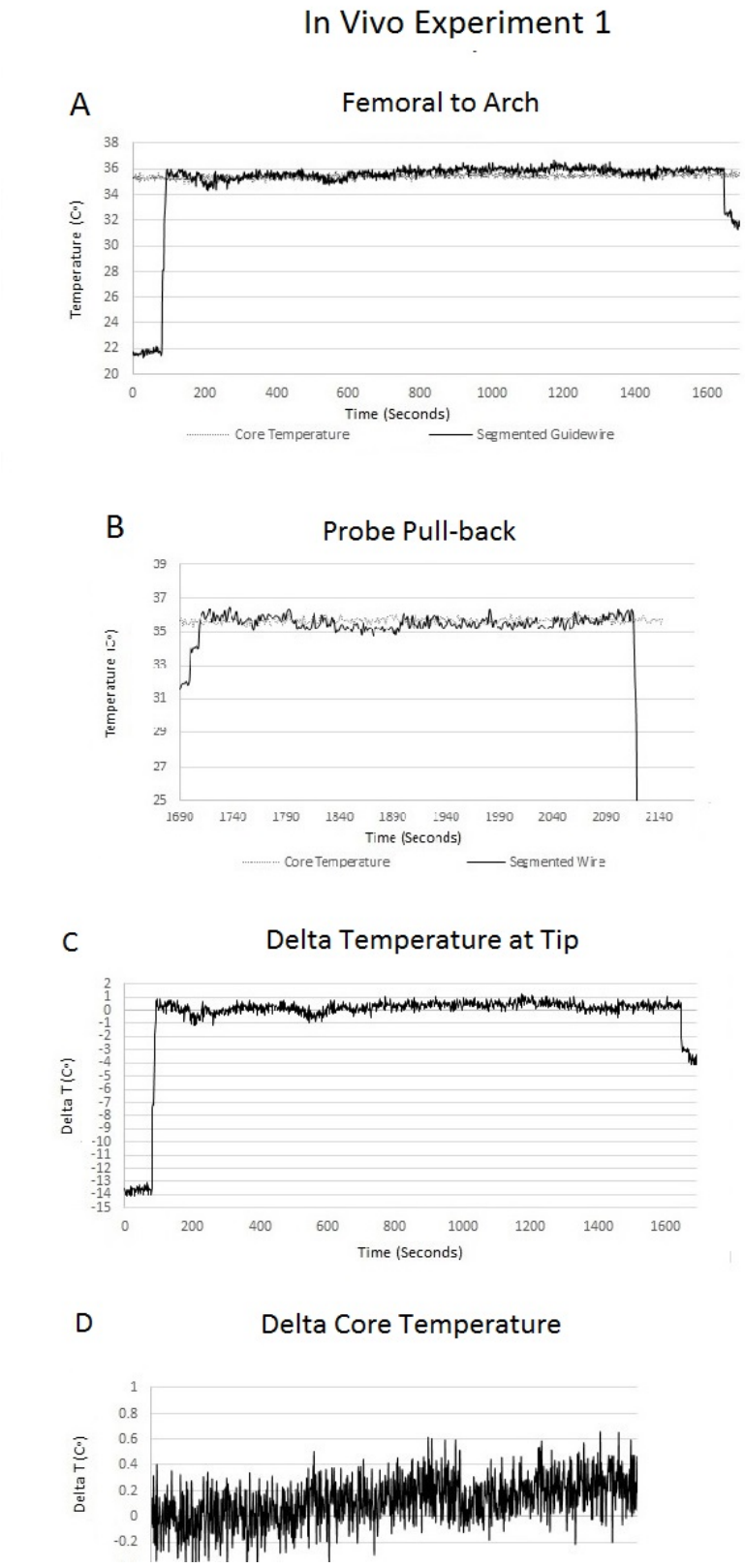

Figure 4.8 Temperature measured at the tip of the 260 cm segmented nitinol guidewire during left heart catheterization in swine. The guidewire is introduced from the femoral artery and advanced to the aortic arch (a). The temperature probe is pulled back while guidewire tip is held stationary at the arch to confirm no heating occurs along the guidewire shaft (b). Temperature changes are clinically negligible (c). Core temperature of the animal increased by 0.4°C during the procedure (t=35 mins) (d).

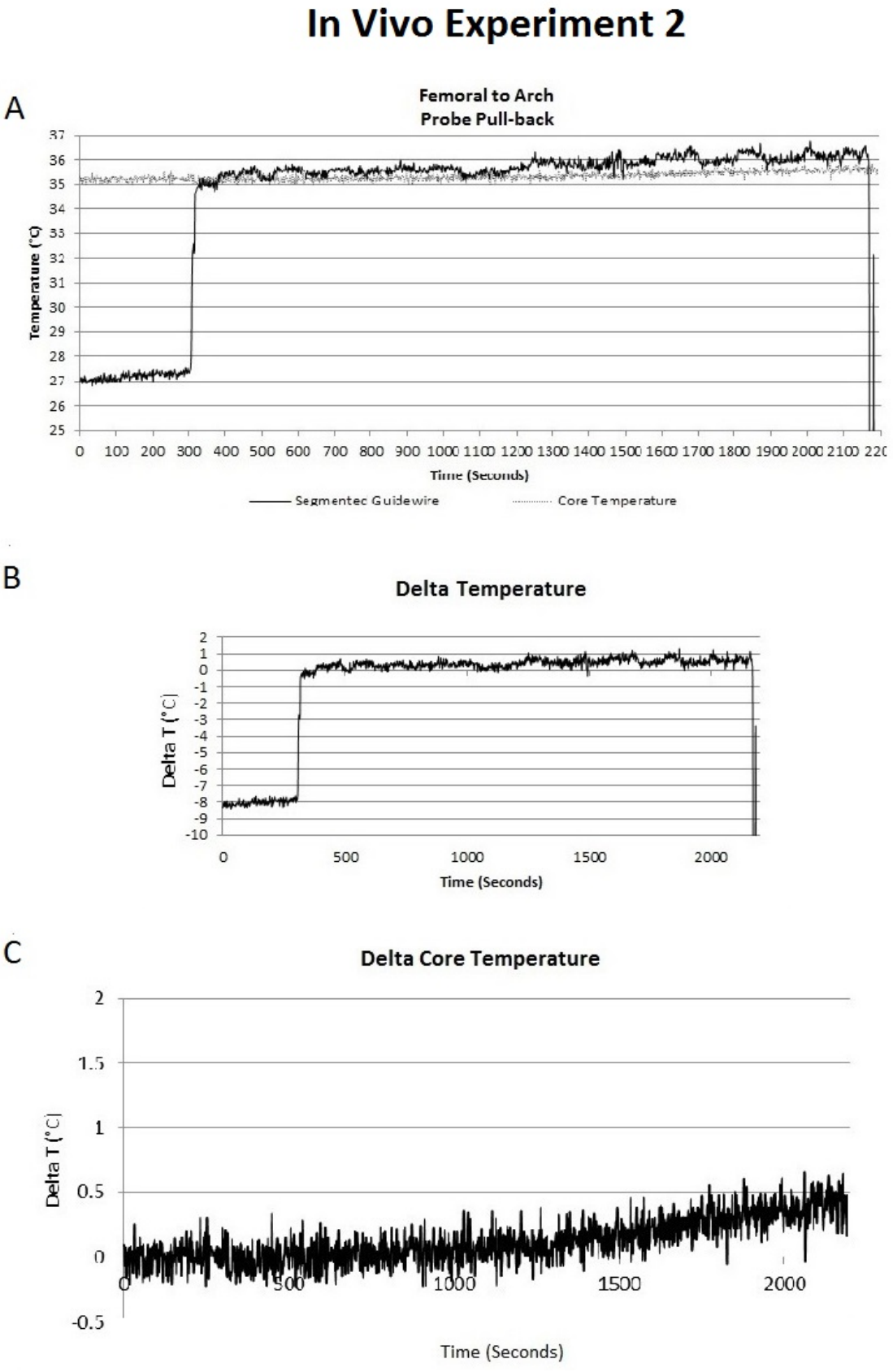

Figure 4.9 Temperature measured at the tip of the 260 cm segmented nitinol guidewire (a), and the core temperature of the animal (b). Weight=63 kg

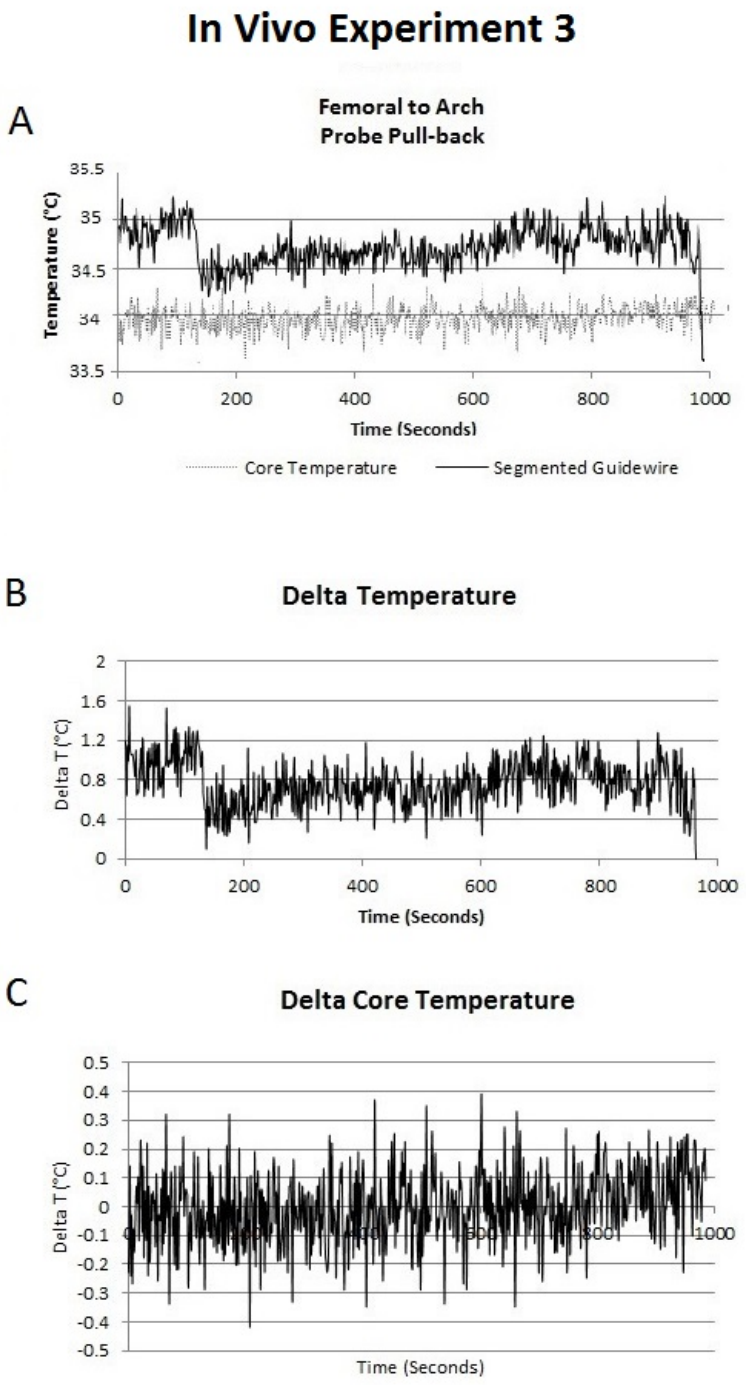

Figure 4.10 Temperature measured at the tip of the 260 cm segmented nitinol guidewire when advancing the guidewire from femoral artery to the arch during left heart catheterization on a small pig (weight= 24 kg) (a).Changes in temperature at the tip (b) and the core temperature (c) are negligible.

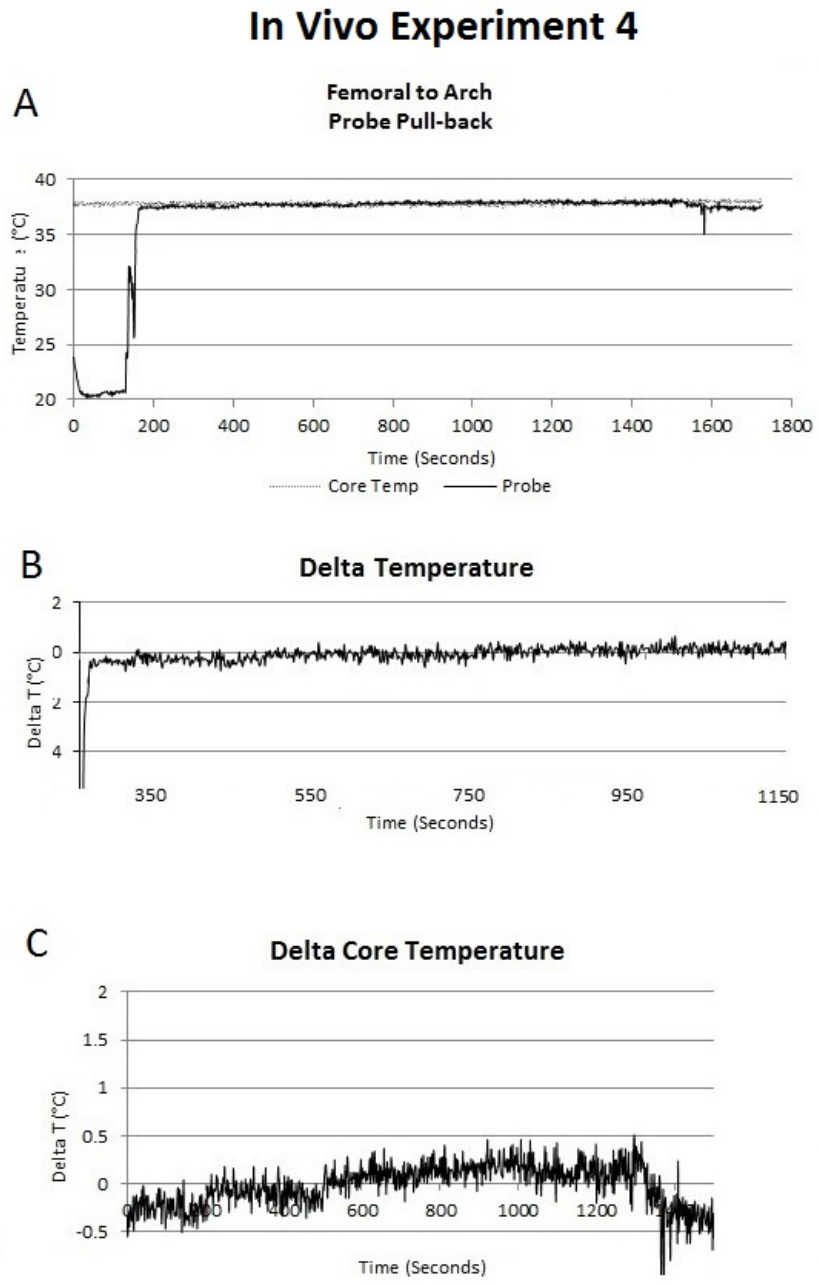

Figure 4.11 Temperature measured at the tip of the 260 cm segmented nitinol guidewire during left heart catheterization on swine (weight= 27kg).

5. DISCUSSION

5.1 Mechanical Performance

Mechanical competence is a key feature expected of a guidewire in order for it to perform according to its intended use. To the authors knowledge, efforts towards a clinically applicable MR-safe guidewire design with preserved mechanical properties have been unsuccessful thus far, despite numerous attempts. Many groups have realized designs that successfully restrict RF-induced temperature elevation at guidewire tip [10, 11, 12, 43]; unfortunately, these designs are inapplicable to the clinic due to their mechanical limitations. Active devices incorporate additional elements into the guidewire design for RF-safety, enhanced visualization or tracking purposes, while passive devices avoid the use of metallic parts to eliminate heating. In case of active devices, the additional components, e.g. transformers, RF chokes, tend to add robustness to the guidewire profile, which reflects as an augmented profile as well as altered stiffness and flexibility of the device, and translates into clinically impracticality. On the other hand, polymer guidewires perform nowhere near their metallic counterparts.

The MR-safe design proposed in this study is both RF-safe and mechanically adequate. It is unique in its simplicity and practicality. The utmost advantage of the design presented here is that it permits the use of non-ferrous metallic components to preserve the mechanical features of conventional guidewires. The use a non-metallic braiding imparts torque transmission, kink-resistance, torquability, and stiffness. The braiding component also provides good support and trackability in vivo. These key qualities lack in other passive MR-safe guidewires, e.g. polymer guidewires, which avoid using metal parts altogether. Contrary to complex active device designs that incorporate additional elements for visualization or RF-safety purposes, the segmented niti-

nol guidewire relies on simple, insulated stiffness-matched components to create a non-conductive metallic core that is free from heating.

In terms of its mechanical performance, the segmented guidewire design has performed similarly to commercially available Glidewire as demonstrated by pushability and torquability tests in vitro. Pushability test was largely affected by the tip design and the outer profile of the tested samples. Tip flexibility tests indeed show variation between the tip profiles of the MR-safe guidewire and the Glidewire. The MR-safe segmdented guidewire tip imparts forces in the same range as a Glidewire, however, it affords optimization. A similar deflection-force profile would enable smoother device tracking within the vasculature. Moreover, steerability and pushability are largely affected by tip flexibility. Its optimization, therefore, would minimize risk of injury to the vasculature, and may expand the guidewire applicability for a wider range of operations (i.e. right heart catheterization). Nevertheless, preliminary in vivo left heart catheterization trials have confirmed that the device is pushable and trackable within swine anatomy. The segmented device was found to be both torquable and maneuverable overall, and the operator was able to deliver the device to the desired location successfully.

5.2 RF-Induced Heating Performance

The initial RF-induced phantom tests were conducted on the preliminary prototypes, namely, the 123-cm segmented guidewire with a 13-cm distal tip segment, and the 120-cm segmented guidewire with the shortened ($<$10 cm) distal tip segment. The purpose was to confirm that by reducing the length of the electrically isolated tip segment of the nitinol guidewire from 13 cm to below that of one quarter wavelength for the tissue under 1.5T ($<$10 cm), heating observed at the tip would be diminished. The results indeed show that temperature increase at the tip was reduced from an average of 3.5 °C to 1.6 °C

(Figure 4.4) in a minimally dissipative, no-flow viscous solution at a 75° flip angle. Further in vitro heating tests performed on a 260-cm segmented guidewire prototype matching the length of standard commercially available guidewires demonstrate that the guidewire exhibits minimal heating. The temperature increase at the tip during 60-second scans has consistently been under 2 °C in compliance with standards [39]. This is in comparison to 13°C observed at the tip of a 260 cm Glidewire (Figure 4.5).

It is known that maximum heating occurs at the tip of long, metallic conductors under MR, as explained in Section 2. Nevertheless, a probe pull-back test was performed to ensure that the connectors do not create capacitance, which may result in excessive heating. This also served to check for possible manufacturing faults and defects that might have occurred during handling the device, which might compromise electrical insulation of the connected segments to create conductive structures exceeding the resonant length. The probe pull-back test confirmed negligible heating at the connectors (Figure 4.5). Contrary to active devices where hot spots do not disappear but shift their location, probe pull-back tests confirmed that the insulated connectors do not create hot spots along the shaft.

As explained in Section 2.1, there are several mechanisms that contribute to RF-induced heating in the MR environment. This study shows heating of long guidewires due to standing wave formation is eradicated by segmenting the core of the guidewire. The temperature increase observed at the tip of the segmented guidewire during heating tests may in fact be independent of the guidewire due to the heating of the minimally dissipative media itself. The temperature increase observed at the tip of the segmented guidewire may be attributed in part to the eddy currents induced in the gel by the E-field. During phantom tests the tip of the guidewire is placed at an off-center position where this E-field is higher to create worst-case heating conditions.

The E-field is augmented closer to the bore of the scanner, and the consequent heating is higher at this region because coupling occurs between to the E-field of the transmit coil and the wire. A test set up was created to monitor the temperature increase at an off-center position in the gel without placing a guidewire or any other conductive material within it. A 0.5°C temperature increase of the gel (Figure 4.6) was recorded. This is in agreement with the findings of other groups who have investigated heating of conductive parts in MRI due to RF-induced heating. For example, Dempsey et al. proposed that the excessive temperature increase observed during MRI scans where long, conductive components are involved is mainly due to the antenna effect, and partly due to other mechanisms. Maximum recorded temperature rises were 0.6°C for the loop, and 63.5°C for the resonant antenna [48].

In Vivo Catheterization and Heating Performance

The segmented device was found torquable and maneuverable overall during left heart catheterization experiments (n=7). The operator was able to deliver the device to the aortic arch successfully in all cases. Only during one out of the seven cases the operator was unable to enter the left ventricle. The unsuccessful attempt may be partly attributed to the fact that the device was re-sterilized and re-used after each test, even though guidewires are intended for single use only. The excessive use of the device may have affected the shape of the tip. Moreover the procedures were performed without the aid of a catheter as would be during a typical routine catheterization. This reflects as the lack of additional mechanical support to the guidewire, which in return impairs the steerability of the guidewire. Optimization of the tip geometry and performing in vivo experiments with a catheter would potentially improve mechanical performance and enable a wider range of operational applications.

In vivo heating tests were conducted on four animals. No detectable

heating was found at the tip of the guidewire during catheterization, regardless of the weight of the animals (n=2, avg weight=25.5 kg; n=2, avg weight=50.5 kg). Probe pull-back tests detected no heating along the shaft of the device (Figure 4.8A; Figures 4.9B, 4.10B, 4.11B). In vivo heating data clearly differs from those obtained from phantom tests. During in vivo procedures heating is expected to be less prominent, because contrary to in vitro heating experiments which were performed in a non-flow solution with minimally thermally dissipative properties, there is blood flow which may cool the vicinity of the guidewire. Furthermore, phantom tests were conducted using a non-clinical flip angle (75°) as opposed to the typical 45° for in vivo procedures. It is known that temperature increases with the square of the flip angle. In vivo studies indeed show that in addition to the blood flow which reduces the heating effect, by using a low flip angle (45°) heating at the tip is further reduced (Table 5.1). The results show that temperature rise both at 45° and 75° flip angle is well below the safety limit of 2°C.

Similar to the in vitro tests, some heating, though negligible, is observed at the tip of the guidewire. The averaged temperature difference between the tip of the guidewire and the core temperature of the animal was <0.3 °C throughout catheterization (t= 35 min). The post-scan core temperature was 0.4 °C higher than the average pre-scan core temperature. Other studies report similar findings of temperature changes up to 0.6°C in patients undergoing clinical MR procedures [47]. This can be attributed to the non-resonant induction mechanism. Due to the non-homogeneous conductive patterns encountered during interventional procedures, RF power is unevenly distributed in the body and may result in excessive RF energy accumulation in certain locations during an MRI scan [49]. This suggests that heating may be observed independent of the guidewire due to RF-induced tissue heating [47], but may be expected to intensify upon introduction of guidewires into the close vicinity of these RF-

induced hot spots [49]. In agreement with this rationale, when the core temperature was recorded without a guidewire in the vasculature, an increase by 0.1 °C and 0.4 °C were recorded at 45° and 75° flip angles, respectively (t=35 min) (Table 5.1).

Table 5.1
Temperature measurements acquired during in vivo RF-induced heating tests (t=35 minutes)

	With Guidewire		**No Guidewire**	
Flip Angle (°)	45	75	45	75
Average baseline temperature (°C)	35.35	35.4	35.85	36.14
Average Δ Temperature (°C)	0.36	1.00	0.11	0.38

5.3 Guidewire Conspicuty Under MR

An advantage of the MR-safe guidewire design proposed here is that the segmented-core design of the guidewire does not permit heating even at higher flip angles. Therefore high contrast images are attainable without risking RF-induced heating. Even still, perhaps the most deficient feature of the segmented device compared to the alternative MR-safe designs is its conspicuity. Though the susceptibility artifacts created by the markers are adequate for visualization and tracking in vivo, a shortcoming of the negative contrast created by the iron oxide nanoparticles is that the signal void created by the iron oxide interferes with tissue visualization, which may be undesirable during catheterization. For this reason, the effect of varying core sizes on image artifacts was quantified in vitro in terms of CNR and susceptibility artifact (Table 4.2), and evaluated qualitatively by physicians prior to the application onto the guidewire shaft. Magnetite nanoparticles with core diameters ranging from 70-150nm were incorporated into the final guidewire design for passive visualization of the device during animal catheterization experiments. In vivo images acquired during animal experiments confirmed conspicuity and trackability of the device in swine both at high and low flip angles. Nevertheless, careful quantification of a

comparator device for marker artifact characteristics must be established for its optimization.

6. CONCLUSION

This work demonstrates the feasibility of an intrinsically MR-safe nitinol guidewire design. It is demonstrated that by segmenting the core of the guidewire to reduce the length of each of the linear metallic component to less than one quarter wavelength of resonance frequency at 1.5T, standing wave formation, and ultimately, RF-induced heating can be eliminated. It is further demonstrated that segmentation of the metallic core virtually has no significant effect on the mechanical performance of the device.

In comparison to active devices which implement additional elements into their designs to circumvent heating, this segmented-core design suggests clinical practicality as it does not require an electrical connection to the scanner, which allows for easy intra-operative handling. This may also translate into a wider range of clinical applicability. Additionally, while active designs are often restricted in terms of their design (i.e. length, profile), the simple and design of the segmented guidewire may allow for modifications to its mechanical and physical features as is required by clinican' needs. In vitro and in vivo tests demonstrate that the device performs comparably to commercially available XRF guidewires in terms of its mechanical properties. Because of its simple design,

Aside from electromagnetic and mechanical properties of the device, an equally important criterion defined for the guidewire design was conspicuity. It is shown here that the image artifact created by the iron oxide markers incorporated onto the guidewire tip is satisfactory for passive visualization of the device in vivo during heart catheterization.

It may be concluded that the segmented nitinol-core guidewire is MR-safe. It fulfills the mechanical and MR-safety requirements imposed by international standards [36, 38, 39, 52]. Its conspicuity under MRI is sufficient for diagnostic heart catheterization purposes and its segmented core avoids RF-induced heating yet maintains its mechanical integrity. It is shown that the MR-safe guidewire is comparable to its commercially available MR-unsafe counterparts in terms of its mechanical properties. A guidewire design that is suitable for use under MR is

proposed, which is expected to have significant clinical relevance.

7. FUTURE WORK

It is demonstrated that the mechanical features of the device were adequate for successful completion of left heart catheterization in swine; however, it is acknowledged that its tip flexibility affords optimization. Modification of the tip according to device application will improve device steerability, pushability and trackability in vivo. An increased steerability and trackability ultimately increases the range of operational applications. It may be beneficial for performing right heart catheterization, which requires a more distinct tip shape, for example.

Regarding RF-safety, although in vitro phantom tests and preliminary animal catheterization experiments confirm RF safety of our design, prolonged catheterization studies may be performed to gather extensive heating data in vivo to investigate common occurrences such as coiling of the guidewire tip within the pericardium: curves and kinks result in an uneven distribution of the E-field which consequently may result in excessive heating unaccounted for during our studies. It is worth noting that in vivo heating tests were performed without a catheter as is typical of routine catheterization procedures. The use of a catheter was omitted because the temperature probe affixed to the guidewire during these tests augments device profile. This, together with the additional insulation (provided by a catheter over the guidewire), may affect electromagnetic properties of the guidewire, and consequently the guidewire's heating behavior. However, it may be predicted that this effect will be trivial, as no detectable temperature increase was measured at the tip of the guidewire while it was located within the introducer sheath (Pinnacle, Terumo, 5F). Similar to a catheter, the introducer sheath also provides insulation and may affect heating properties of the guidewire. Additionally, the introducer sheath was at the edge of the scanner bore, which exacerbates heating. As the guidewire was advanced to the aortic arch and into the left ventricle, the temperature rise at the tip was well below the safety limit of 2°C (Table 5.1).

Moreover, an additional outer structure over the guidewire would provide support to the guidewire, which may offer operational benefits such as improved steer-

ability and pushability. In vivo trials comprising introduction of the guidewire using a catheter would enable testing the mechanical capabilities of the segmented guidewire design in aggressive scenarios, such as coiling within the pericardium or right heart catheterization, is therefore a condition for future evaluation.

An aspect that needs further optimization in the segmented guidewire design is conspicuity. The marker design was based on quantification of various features (i.e. CNR, susceptibility artifact size) obtained from different marker types, all of which were evaluated qualitatively. Establishing a commercial device as target to quantify marker features would be beneficial in optimizing conspicuity under MRI.

APPENDIX A. Guidewire characteristics.

Table A.1
Typical design characteristics of commercial guidewires, test methods, and relevant standards

Design Requirement		**Test Method**	**Standard**
Outer diameter	0.035"	Catheter compatibility	FDA Guidance Document Coronary and Cerebrovascular Guidewire
Effective length	260 cm	Catheter compatibility	FDA Guidance Document Coronary and Cerebrovascular Guidewire
Mechanical requirements	Pushability, Torquability, Stiffness, Column strength	Image artifact	ISO 10555-1:1995 "Sterile, single-use intravascular catheters - Part 1: General Requirements"
Atraumatic tip	Softness, tip geometry	Tip flexiblity Steerability	ISO 10555-1:1995 "Sterile, single-use intravascular catheters - Part 1: General Requirements"
Passive visualization by negative contrast	Contrast-to-noise ratio, Susceptibility artifact	Image artifact	ASTM-F2119 "Standard Test Methods for Evaluation of MR Image Artifacts from Passive Implants"
RF Safety	<2 °C	In Vitro/In Vivo RF-Induced heating tests	ASTM F2182-02a "Standard Test Method for measurement of radiofrequency induced heating near passive passive implants during magnetic resonance imaging"

REFERENCES

1. Halabi, M., A. Z. Faranesh, W. H. Schenke, V. J. Wright, M. S. Hansen, C. E. Saikus, O. Kocaturk, R. J. Lederman, and K. Ratnayaka, "Real-time cardiovascular magnetic resonance subxiphoid pericardial access and pericardiocentesis using off-the-shelf devices in swine," *J Cardiovasc Magn Reson*, Vol. 15, no. 61, p. 20, 2013.

2. Halabi, M., K. Ratnayaka, A. Z. Faranesh, M. S. Hansen, I. M. Barbash, M. A. Eckhaus, J. R. Wilson, M. Y. Chen, M. C. Slack, O. Kocaturk, *et al.*, "Transthoracic delivery of large devices into the left ventricle through the right ventricle and interventricular septum: preclinical feasibility.," *Journal of cardiovascular magnetic resonance: official journal of the Society for Cardiovascular Magnetic Resonance*, Vol. 15, no. 1, pp. 10–10, 2012.

3. Ratnayaka, K., A. Z. Faranesh, M. S. Hansen, A. M. Stine, M. Halabi, I. M. Barbash, W. H. Schenke, V. J. Wright, L. P. Grant, P. Kellman, *et al.*, "Real-time mri-guided right heart catheterization in adults using passive catheters," *European heart journal*, p. ehs189, 2012.

4. Saikus, C. E., K. Ratnayaka, I. M. Barbash, J. H. Colyer, O. Kocaturk, A. Z. Faranesh, and R. J. Lederman, "Mri-guided vascular access with an active visualization needle," *Journal of Magnetic Resonance Imaging*, Vol. 34, no. 5, pp. 1159–1166, 2011.

5. Nitz, W. R., A. Oppelt, W. Renz, C. Manke, M. Lenhart, and J. Link, "On the heating of linear conductive structures as guide wires and catheters in interventional mri," *Journal of Magnetic Resonance Imaging*, Vol. 13, no. 1, pp. 105–114, 2001.

6. Rogers, T., K. Ratnayaka, and R. J. Lederman, "Mri catheterization in cardiopulmonary disease," *CHEST Journal*, Vol. 145, no. 1, pp. 30–36, 2014.

7. Dick, A. J., V. K. Raman, A. N. Raval, M. A. Guttman, R. B. Thompson, C. Ozturk, D. C. Peters, A. M. Stine, V. J. Wright, W. H. Schenke, *et al.*, "Invasive human magnetic resonance imaging: feasibility during revascularization in a combined xmr suite," *Catheterization and cardiovascular interventions*, Vol. 64, no. 3, pp. 265–274, 2005.

8. Lederman, R. J., "Cardiovascular interventional magnetic resonance imaging," *Circulation*, Vol. 112, no. 19, pp. 3009–3017, 2005.

9. Schulz, T., S. Puccini, J.-P. Schneider, and T. Kahn, "Interventional and intraoperative mr: review and update of techniques and clinical experience," *European radiology*, Vol. 14, no. 12, pp. 2212–2227, 2004.

10. Mekle, R., E. Hofmann, K. Scheffler, and D. Bilecen, "A polymer-based mr-compatible guidewire: A study to explore new prospects for interventional peripheral magnetic resonance angiography (ipmra)," *Journal of Magnetic Resonance Imaging*, Vol. 23, no. 2, pp. 145–155, 2006.

11. Weiss, S., P. Vernickel, T. Schaeffter, V. Schulz, and B. Gleich, "Transmission line for improved rf safety of interventional devices," *Magnetic resonance in medicine*, Vol. 54, no. 1, pp. 182–189, 2005.

12. Wolska-Krawczyk, M., M. A. Rube, E. Immel, A. Melzer, and A. Buecker, "Heating and safety of a new mr-compatible guidewire prototype versus a standard nitinol guidewire," *Radiological physics and technology*, Vol. 7, no. 1, pp. 95–101, 2014.

13. Armenean, C., E. Perrin, M. Armenean, O. Beuf, F. Pilleul, and H. Saint-Jalmes, "Rf-induced temperature elevation along metallic wires in clinical magnetic resonance imaging: Influence of diameter and length," *Magnetic Resonance in Medicine*, Vol. 52, no. 5, pp. 1200–1206, 2004.

14. Bassen, H., W. Kainz, G. Mendoza, and T. Kellom, "Mri-induced heating of selected thin wire metallic implants-laboratory and computational studies-findings and new questions raised," *Minimally Invasive Therapy & Allied Technologies*, Vol. 15, no. 2, pp. 76–84, 2006.

15. Gray, R. W., W. T. Bibens, and F. G. Shellock, "Simple design changes to wires to substantially reduce mri-induced heating at 1.5 t: implications for implanted leads," *Magnetic resonance imaging*, Vol. 23, no. 8, pp. 887–891, 2005.

16. Ladd, M. E., and H. H. Quick, "Reduction of resonant rf heating in intravascular catheters using coaxial chokes," *Magnetic resonance in medicine*, Vol. 43, no. 4, pp. 615–619, 2000.

17. Konings, M. K., L. W. Bartels, H. F. Smits, and C. J. Bakker, "Heating around intravascular guidewires by resonating rf waves," *Journal of Magnetic Resonance Imaging*, Vol. 12, no. 1, pp. 79–85, 2000.

18. Liu, C.-Y., K. Farahani, D. S. Lu, G. Duckwiler, and A. Oppelt, "Safety of mri-guided endovascular guidewire applications," *Journal of Magnetic Resonance Imaging*, Vol. 12, no. 1, pp. 75–78, 2000.

19. Yeung, C. J., R. C. Susil, and E. Atalar, "Rf heating due to conductive wires during mri depends on the phase distribution of the transmit field," *Magnetic Resonance in Medicine*, Vol. 48, no. 6, pp. 1096–1098, 2002.

20. Eryaman, Y., B. Akin, and E. Atalar, "Reduction of implant rf heating through modification of transmit coil electric field," *Magnetic Resonance in Medicine*, Vol. 65, no. 5, pp. 1305–1313, 2011.

21. Nordbeck, P., F. Fidler, I. Weiss, M. Warmuth, M. T. Friedrich, P. Ehses, W. Geistert, O. Ritter, P. M. Jakob, M. E. Ladd, *et al.*, "Spatial distribution of rf-induced e-fields and implant heating in mri," *Magnetic Resonance in Medicine*, Vol. 60, no. 2, pp. 312–319, 2008.

22. Settecase, F., S. W. Hetts, A. J. Martin, T. P. Roberts, A. F. Bernhardt, L. Evans, V. Malba, M. Saeed, R. L. Arenson, W. Kucharzyk, *et al.*, "Rf heating of mri-assisted catheter steering coils for interventional mri," *Academic radiology*, Vol. 18, no. 3, pp. 277–285, 2011.

23. Yeung, C. J., P. Karmarkar, and E. R. McVeigh, "Minimizing rf heating of conducting wires in mri," *Magnetic Resonance in Medicine*, Vol. 58, no. 5, pp. 1028–1034, 2007.

24. Yeung, C. J., R. C. Susil, and E. Atalar, "Rf safety of wires in interventional mri: using a safety index," *Magnetic Resonance in Medicine*, Vol. 47, no. 1, pp. 187–193, 2002.

25. Ocali, O., and E. Atalar, "Intravascular magnetic resonance imaging using a loopless catheter antenna," *Magnetic resonance in medicine*, Vol. 37, no. 1, pp. 112–118, 1997.

26. Quick, H. H., M. O. Zenge, H. Kuehl, G. Kaiser, S. Aker, S. Massing, S. Bosk, and M. E. Ladd, "Interventional magnetic resonance angiography with no strings attached: wireless active catheter visualization," *Magnetic resonance in medicine*, Vol. 53, no. 2, pp. 446–455, 2005.

27. Hegde, S., M. E. Miquel, R. Boubertakh, D. Gilderdale, V. Muthurangu, S. F. Keevil, I. Young, D. L. Hill, and R. S. Razavi, "Interactive mr imaging and tracking of catheters with multiple tuned fiducial markers," *Journal of vascular and interventional radiology*, Vol. 17, no. 7, pp. 1175–1179, 2006.

28. Kocaturk, O., A. H. Kim, C. E. Saikus, M. A. Guttman, A. Z. Faranesh, C. Ozturk, and R. J. Lederman, "Active two-channel 0.035 ^{3} guidewire for interventional cardiovascular mri," *Journal of Magnetic Resonance Imaging*, Vol. 30, no. 2, pp. 461–465, 2009.

29. Susil, R. C., C. J. Yeung, and E. Atalar, "Intravascular extended sensitivity (ives) mri antennas," *Magnetic resonance in medicine*, Vol. 50, no. 2, pp. 383–390, 2003.

30. Ladd, M. E., P. Erhart, J. F. Debatin, E. Hofmann, P. Boesiger, G. K. Von Schulthess, and G. C. McKinnon, "Guidewire antennas for mr fluoroscopy," *Magnetic resonance in medicine*, Vol. 37, no. 6, pp. 891–897, 1997.

31. Bakker, C., C. Bos, and H. Weinmann, "Passive tracking of catheters and guidewires by contrast-enhanced mr fluoroscopy," *Magnetic resonance in medicine*, Vol. 45, no. 1, pp. 17–23, 2001.

32. Mueller, R. L., and T. A. Sanborn, "The history of interventional cardiology: cardiac catheterization, angioplasty, and related interventions," *American heart journal*, Vol. 129, no. 1, pp. 146–172, 1995.

33. King, S. B., "The development of interventional cardiology," *Journal of the American College of Cardiology*, Vol. 31, no. 4s2, pp. 64B–88B, 1998.

34. Lange, R. A., and L. D. Hillis, "Diagnostic cardiac catheterization," *Circulation*, Vol. 107, no. 17, pp. e111–e113, 2003.

35. "ASTM-F2119 Standard Test Method for Evaluation of MR Image Artifacts from Passive Implants."

36. *ISO 11070:1998 Sterile, single-use intravascular catheter introducers.*

37. Bock, M., R. Umathum, J. Sikora, S. Brenner, E. Aguor, and W. Semmler, "A faraday effect position sensor for interventional magnetic resonance imaging," *Physics in medicine and biology*, Vol. 51, no. 4, p. 999, 2006.

38. "A Primer On Medical Device Interactions with Magnetic Resonance Imaging Systems, Draft Document, FDA, Center for Devices and Radiological Health ."

39. "FDA Guidance for Industry: Guidance for the Submission Of Premarket Notifications for Magnetic Resonance Diagnostic Devices."

40. Duerk, J. L., E. Y. Wong, and J. S. Lewin, "A brief review of hardware for catheter tracking in magnetic resonance imaging," *Magnetic Resonance Materials in Physics, Biology and Medicine*, Vol. 13, no. 3, pp. 199–208, 2001.

41. Weiss, S., T. Kuehne, F. Brinkert, G. Krombach, M. Katoh, T. Schaeffter, R. W. Guenther, and A. Buecker, "In vivo safe catheter visualization and slice tracking using an optically detunable resonant marker," *Magnetic resonance in medicine*, Vol. 52, no. 4, pp. 860–868, 2004.

42. "ASTM-F2182-02a: Standard Test Method for Measurement of Radio Frequency Induced Heating Near Passive Implants During Magnetic Resonance Imaging."

43. Vernickel, P., V. Schulz, S. Weiss, and B. Gleich, "A safe transmission line for mri," *Biomedical Engineering, IEEE Transactions on*, Vol. 52, no. 6, pp. 1094–1102, 2005.

44. Sonmez, M., C. E. Saikus, J. A. Bell, D. N. Franson, M. Halabi, A. Z. Faranesh, C. Ozturk, R. J. Lederman, and O. Kocaturk, "Mri active guidewire with an embedded temperature probe and providing a distinct tip signal to enhance clinical safety," *J Cardiovasc Magn Reson*, Vol. 14, p. 38, 2012.

45. Stephen, Z. R., F. M. Kievit, and M. Zhang, "Magnetite nanoparticles for medical mr imaging," *Materials Today*, Vol. 14, no. 7, pp. 330–338, 2011.

46. Huang, J., X. Zhong, L. Wang, L. Yang, and H. Mao, "Improving the magnetic resonance imaging contrast and detection methods with engineered magnetic nanoparticles," *Theranostics*, Vol. 2, no. 1, p. 86, 2012.

47. Shellock, F. G., and J. V. Crues, "Mr procedures: Biologic effects, safety, and patient care 1," *Radiology*, Vol. 232, no. 3, pp. 635–652, 2004.

48. Dempsey, M. F., B. Condon, and D. M. Hadley, "Investigation of the factors responsible for burns during mri," *Journal of Magnetic Resonance Imaging*, Vol. 13, no. 4, pp. 627–631, 2001.

49. Shellock, F. G., "Radiofrequency energy-induced heating during mr procedures: A review," *Journal of Magnetic Resonance Imaging*, Vol. 12, no. 1, pp. 30–36, 2000.

50. Yeung, C. J., and E. Atalar, "A greenâs function approach to local rf heating in interventional mri," *Medical physics*, Vol. 28, no. 5, pp. 826–832, 2001.

51. "FDA Coronary and Cerebrovascular Guidewire guidance document."

52. "ISO10555-1:1995 Intravascular catheters – Sterile and single-use catheters – Part 1: General requirements."